DOCTORAL DISSERTATION

A STUDY OF MODELING SHIP'S COLLISION AVOIDANCE ACTION USING PREDICTIVE ALGORITHMS

March 2024

Graduate School of Marine Science and Technology
Tokyo University of Marine Science and Technology
Doctoral Course of Applied Marine Environmental Studies

SONG JAEYOUNG

DOCTORAL DISSERTATION

A STUDY OF MODELING SHIP'S COLLISION AVOIDANCE ACTION USING PREDICTIVE ALGORITHMS

March 2024

Graduate School of Marine Science and Technology
Tokyo University of Marine Science and Technology
Doctoral Course of Applied Marine Environmental Studies

SONG JAEYOUNG

Contents

List of Figures i
List of Tables iii

1 Introduction **1**
1.1 Research background 1
1.1.1 Collision accident 1
1.1.2 Decision making for collision avoidance 5
1.1.2.1 Flows of decision making 5
1.1.2.2 Modeling of collision risk and avoidance 5
1.2 Objective of this dissertation 7
1.3 Structure of this dissertation 8

2 Calculation of the relationship between the ships **10**

3 Modeling ship's collision avoidance direction in an encounter situation **14**
3.1 Objective of this work 14
3.2 Materials and methods 15
3.2.1 Collision avoidance 15
3.2.1.1 Collision avoidance algorithm 16
3.2.2 Data acquisition 20
3.2.2.1 Data collection 20
3.2.2.2 Data processing 22
3.2.3 Ensemble model 26
3.2.3.1 Base model 27
3.2.3.2 Bagging and AdaBoost model 28
3.2.3.3 Hyperparameters and model assessment 29
3.3 Result 33
3.3.1 Result of data analysis 33
3.3.2 Result of model construction 36

3.3.2.1 Construction result . . . 36
3.3.2.2 Validation result . . . 37
3.4 Discussion . . . 39
3.4.1 Discussion of variables and models . . . 39
3.4.2 Discussion of results . . . 41

4 Modeling ship's encounter situation awareness result 43
4.1 Objective of this work . . . 43
4.2 Materials and methods . . . 44
4.2.1 Risk of collision . . . 45
4.2.1.1 Collision Risk Index . . . 45
4.2.1.2 Scenarios of collision . . . 48
4.2.2 Acquisition of experimental data . . . 49
4.2.2.1 Interviewing . . . 49
4.2.2.2 Data processing . . . 50
4.2.3 Modeling . . . 51
4.2.3.1 Support Vector Machine . . . 51
4.2.3.2 Hyperparameters . . . 53
4.2.3.3 Verification of model . . . 54
4.3 Result . . . 57
4.3.1 Results of data acquisition . . . 57
4.3.1.1 Calculation results of Collision Risk . . . 57
4.3.1.2 Results of data acquisition . . . 59
4.3.2 Results of modeling . . . 61
4.3.2.1 Estimation results of modeling . . . 61
4.3.2.2 Validation result of modeling . . . 62
4.4 Discussion . . . 64

5 Conclusion 66
Bibliography . . . 75

A The outputs of the proposed models 76
A.1 The overview of the model illustrated in Chapter 3 . . . 76
A.2 The Output of the model illustrated in Chapter 3 . . . 77
A.3 The overview of the model illustrated in Chapter 4 . . . 78
A.4 The Output of the model illustrated in Chapter 4 . . . 78

Acknowledgments 80

List of Figures

1.1 The encounter situations defined by COLREGs. **(a)**, head-on , **(b)**, stand-on of crossing situation, **(c)**, give-away of crossing situation , **(d)** overtake. 2
1.2 Illustrate of encounter situation. 4
1.3 Structural overview of dissertation. 9

2.1 Representation of the OS and TS parameters within the earth fixed coordinate system. 11

3.1 Flow charts of model construction and validation. 15
3.2 **(a)** Conceptual diagram of OZT with parameters, **(b)** The computed results of OZT. OS's speed 15 kts, course 000deg, Length Over All 150m. TS's speed 10 kts, course 270deg. Az 050deg and the distance of two vessels 3.0 nautical miles. 17
3.3 Geographical visualization of the data collected area (Near Oshima, Japan). 21
3.4 Flow chart of data processing and variable construction. 25
3.5 Illustration of model framework for Bagging (Left), and AdaBoost(Right). 26
3.6 Illustration of confusion matrix for binary classification. 30
3.7 Distribution of the predictor variables. Classes 0 and 1 denote altering course to port and starboard sides, respectively. 34
3.8 ROC and AUC metrics of Bagging model **(a)** and AdaBoost model **(b)**. . 38

4.1 Flow charts of this work. 44
4.2 Illustration of the confusion matrix for Multi-class classification. 55
4.3 Illustration of the confusion matrix for micro-averaging. 56
4.4 Visualization of collision risk matrices in case **(a)**, $V_t < V_o$, **(b)**, $V_t = V_o$, **(c)** $V_t > V_o$. 58
4.5 Distribution of the predictors. Set (Y) denote Head-on(0), Give- away(1), and Stand-on(2), respectively. 60

4.6 The receiver operating characteristic (ROC) curve and area under the curve (AUC) score of the different kernel functions are evaluated in the following cases: **(a)** Linear, **(b)** Polynomial (2nd degree), **(c)** Polynomial (3rd degree), and **(d)** Gaussian (RBF). 63

A.1 Overview of model constructed in Chapter 3 76

A.2 Overview of model constructed in Chapter 4 78

List of Tables

1.1 Variables and parameters employed in the categorization of encounter scenarios. 3

3.1 Description of data and statistical metrics. 33
3.2 Correlation matrix between predictor variables. 35
3.3 Estimation of the optimal hyperparameters for models. 37
3.4 Confusion matrix for high accuracy models. 39

4.1 Weight values for utility function of CRI. 45
4.2 Data description and statistical metrics. 59
4.3 Correlation matrix between the predictors. 59
4.4 Estimation result of the optimal hyperparameters of the each kernel. . . 61
4.5 Confusion matrices for high-performance by kernels of model. 62

A.1 Example of prediction result of optimal model constructed in chapter 3. 77
A.2 Example of prediction result of optimal model constructed in chapter 4. 79

Chapter 1

Introduction

1.1 Research background

Navigators perform duty assignments to ensure safe navigation and prevent maritime accidents. Maritime accidents are classified into 13 categories [1]. The accidents include collisions, contacts, grounding, flooding, et cetera. Among these, collisions are the most frequently occurring type of maritime accident. According to Japan Marine Accident Tribunal(JMAT), collision accidents account for 25% of all accidents[2, 3, 4]. Collision accidents involve the collision itself and give rise to secondary issues like oil spills, casualties, and vessel damage [5, 6, 7, 8]. Therefore, it is essential to find solutions to reduce collision accidents and achieve safe navigation [9]. This section's subsections report definitions of collision accidents, customary practices for collision avoidance, and decision-making in collision avoidance.

1.1.1 Collision accident

A collision accident is a physical collision between encountering vessels [10]. In maritime law, it is defined as an act that causes damage to two or more ships or, people or property on different vessels due to navigational issues [11]. To avoid collision accidents, navigators analyze the situation and consider courses of action. This process applies customary rules known as COLREG (Convention on the International Regulations for Preventing Collision at Sea). COLREG is the fundamental set of rules used in collision avoidance. The rule has 41 regulations across six categories (Part A to F). They instruct navigators to use all available means to detect collision risks (Rule 5: Look-out). Navigators have no restrictions on their means, but some commonly known ones include DCPA(Distance at the Closest Point of Approach), TCPA(Time to DCPA), navigational areas, performance, vessel specifications, speed, and relative

bearing [12]. The factor of individual experience influences the recognition of the risk of conflict using these factors [13]. After recognizing the risk of collision, navigators need to assess the current encounter situation to decide on collision avoidance actions. The customary practices defined in COLREG determine the encounter situation and collision avoidance actions as follows [14].

- Head-on situation (Rule 14, Figure 1.1 (a)): It is considered that a vessel has sighted another vessel directly ahead or nearly ahead. In such a situation, both vessels are required to change their course to the right (starboard) in order to pass each other on the left (port) side.
- Crossing situation (Rule 15, Figure 1.1 (b and c)): It is considered to occur when a ship crosses the path of another. In such instances, the vessel that has the other on its starboard side is required to yield the right of way.
- Overtaking situation (Rule 13, Figure 1.1 (d)): In COLREG terms, a vessel is overtaking another when it approaches from a direction more than 22.5 degrees behind the other vessel's beam. In this scenario, it is expected that any vessel overtaking another should yield the right of way to the vessel being overtaken.

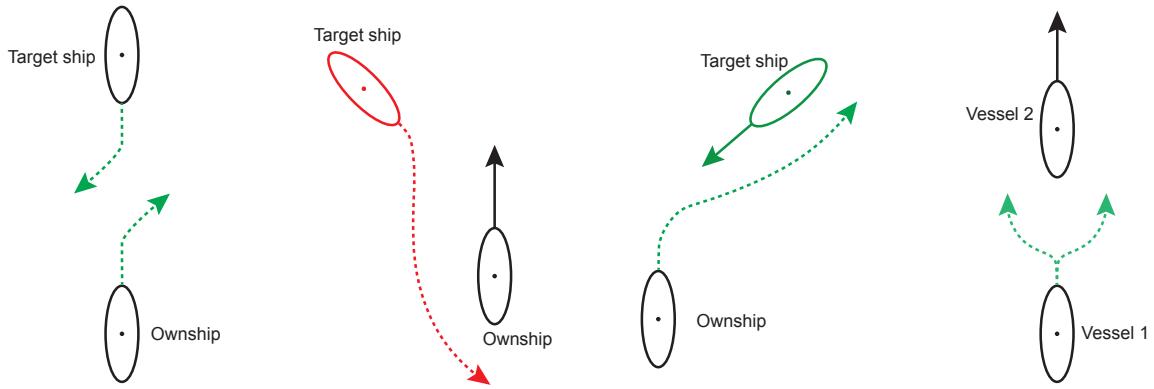

Figure 1.1. The encounter situations defined by COLREGs. **(a)**, head-on , **(b)**, stand-on of crossing situation, **(c)**, give-away of crossing situation , **(d)** overtake.

Figure 1.2 illustrates the encounter situations distinguished by sectors. Here, the coordinate system is relative bearing coordinates with respect to the own ship's center. When the other vessel is in sector 1, the encounter situation is classified as Head-on. If the other vessel is in sector 2, it falls under Crossing with Stand-on situation; if it

is in sector 3, it is classified as Crossing with Give-way. If the other vessel is within the sector of the own ship's masthead lights, it is categorized as Overtaking. Excluding overtaking situations, COLREG applies exceptions to following customary practices (Rule 2) [15]. COLREG does not numerically define the method for distinguishing encounter situations by sectors, as explained in Figure 1.2. However, it mentions an angle for overtaking situations, which is the stern light angle. The angles used to differentiate Head-on and Crossing in Figure 1.2 ($\varphi_1 \sim \varphi_2$) varied slightly in value in each reported paper. These values are documented in Table 1.1. The definitions of the terms used in Table 1.1 are as follows.

- The concept of "Relative Bearing" pertains to the determination of the azimuth angle between the heading of two ships, measured in a clockwise direction from the heading of the observer's ship to the heading of the target ship [16].
- The term "Heading" denotes the orientation of a vessel at a specific point in time, represented as the angular measurement from 000 degrees in a clockwise direction to 360 degrees [16].
- The term "Encounter angle" denotes the angle determined by aligning the heading of the TS(Target Ship) with the initial point of the heading vector of OS(Own Ship) [17].

Table 1.1. Variables and parameters employed in the categorization of encounter scenarios.

	Relative bearing	Heading (OS)	Heading (TS)	Encounter angle	Range Head-on
[18]	√	√	√		337.5 ∼ 022.5
[19]	√	√	√	√	348.75 ∼ 011.25
[20]	√	√	√		345.0 ∼ 015.0
[21]	√	√	√	√	355.0 ∼ 005.0
[22]	√	√	√	√	348.75 ∼ 011.25

Here, the term "Range of Head-on" denotes the specific area value identified as a head-on situation when a target ship (TS) is within a certain range relative to the bearing of the own ship (OS).

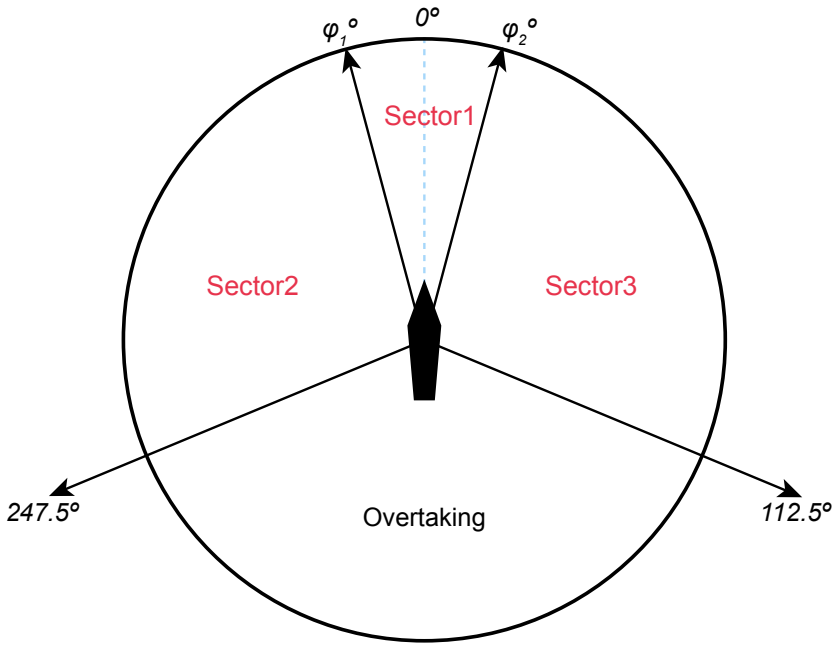

Figure 1.2. Illustrate of encounter situation.

Tam and Bucknall [18] classified the categorization of collision risk encounters with obstacles as an approach based on geographical areas for the development of an evaluation method. Hasegawa et al. [19] and Namgung [22] categorized the regions confronting obstructions into six segments according to the relative orientation of the obstacle in order to develop the algorithm. Yoo and Lee [20] conducted a numerical classification of encounter situations according to the COLREGs in order to validate the environmental stress model, which is a collision risk index. Zhang et al. [21] categorized encounter scenarios by considering spatial areas and angles in order to create a decision making system for collision avoidance. Nevertheless, discrepancies were found in the relative bearings utilized to differentiate between head-on and crossing situations across various studies.

1.1.2 Decision making for collision avoidance

1.1.2.1 Flows of decision making

The navigation officer of a vessel on underway goes through a four-stage decision-making process: information acquisition, situational analysis, decision-making, and action [23]. As reported in Section 1.1.1, navigators analyze the possibility of collision and encounter situations using variables such as DCPA, TCPA, relative bearing, distance, et cetera [14]. Subsequently, they utilize personal skills, conventional rules, and knowledge to make avoidance decisions based on the acquired and analyzed risky situations. The collision prevention rules that form the foundation of specialized knowledge define only basic concepts and principles, allowing exceptions based on on-site judgment [15]. Navigators' situational analysis and decisions are subjective and prone to errors [24, 25]. In particular, there have been reports that navigators' CPA-based situational analysis method when observing ARPA(Automatic Radar Plotting Aids) RADAR is unsuitable for predicting collision risks [26]. This is because human experience and knowledge influence the interpretation of information [15]. This error is reported as a significant cause of collision accidents [15]. Various methods for reducing this error, as well as quantifying collision risks, have been reported.

1.1.2.2 Modeling of collision risk and avoidance

Various studies have been conducted on the establishment of collision avoidance algorithms. Imazu et al. [27] proposed an Obstacle Zone by Target (OZT) model by introducing the concept of safe distance and evaluated OZT according to the situation and speed of encounters with the other ship. Kayano et al. [28] applied a Kalman filter based on the OZT model to predict and evaluate ship movements. Sawada et al. [29] used reinforcement learning to build and evaluate an OZT-based automatic evacuation algorithm. Here, the concept and calculation method of internal OZT was proposed for the first time to solve the shortcomings of the trigonometric function-based OZT calculation process, and the Velocity Obstacle (VO) model was proposed. The VO model is an algorithm developed for robot motion planning [30]. Kuwata et al. [31] applied the VO algorithm to ships and proposed a rule-based collision avoidance algorithm based on COLREG. Huang et al. [32] evaluated the usefulness of the VO algorithm in multi-vessel collision situations. A scenario was constructed to simulate a multi-ship collision, and numerical simulations were performed. Zhang

et al. [21] built and evaluated a rule-based collision avoidance algorithm based on the VO model. Zhang et al. defined the concepts of collision-avoidance actions before the counter situation (CAAB) and collision-avoidance actions in counter situation (CAAI) with the concept of collision avoidance threshold. Contributions have been made to address the problem of over-following rules based on these two variables.

Many exciting reports attempt to quantify the risk of collision. Kearon [33] proposed a computational method that calculates the weights of DCPA and TCPA to generalize the risk of collisions. Lisowski [34] proposed a method to define the risk of collision as a mathematical function of TCPA and DCPA. Ren et al. [35] reported a model that combines membership functions to calculate collision risk based on fuzzy logic using AIS data. Xu and Wang [36] reviewed the basic concepts of collision risk and numerical models for collision risk calculation. Since then, various studies have contributed to performing collision risk evaluation by introducing an evaluation index and determining the weight of the index.

In addition to the above risk calculation, there have also been reports on quantifying the risk of collision by building a ship domain. A ship domain is a generalization of the threshold area where a ship does not allow other ships to enter when entering an encounter situation. The domain model is constructed based on statistically processed ship trajectory data. Since it was first proposed by Fujii and Tanaka [37], researchers have proposed many concepts. Goodwin [38] proposed the concept of a domain with three sectors of different critical points. Coldwell [39] proposed an elliptical model in which OS positions are lop-sided.

Finally, some interesting work has been reported on efforts to build models that reflect the cognitive judgment of navigators. Yim et al. [40] proposed a multiple regression model to quantify human risk perception using Coast Guard vessels. Chen et al. [41] reported a scenario-based study of patterned vessel trajectories using AIS data based on human cognitive judgment in inland waterways. Using simulation data, Xue et al. [42] proposed a human maneuvering decision model. This simulation constructed a scenario for the berthing process near a pier. Xue et al. [43] used scenario-based simulation data to propose a human judgment model based on environmental variables, hull control variables, external forces, and loading conditions in berthing maneuvers. Xue et al. [44] proposed a decision tree model using simulation data to explain collision avoidance decision outcomes in crossing situations occurring near piers in port limit.

1.2 Objective of this dissertation

A review of existing research shows that Vessel collisions are a significant challenge because they cause more than just crashes; they cause disasters. COLREG, a collision avoidance convention, does not provide strict figures, and it has been reported that human subjectivity can be involved due to the existence of exceptions. I have identified the decision flow required for collision avoidance and the potential for human error. I identified reported contributions to reducing human error and quantifying collision avoidance. Some interesting contributions to human cognitive judgment have also been reported. These works have quantified human perception of hazard passage patterns in inland waterways and modeled human maneuvering decisions using a variety of variables. However, it is imperative to address the research needs identified in the aforementioned study.

The first is modeling how humans make collision avoidance decisions. Existing studies do not show the reflection of collision avoidance algorithms on human decisions. Furthermore, efforts to reflect human cognitive judgment have been based on data acquired in complex environments within the navigation system. It has been reported that navigation in this region has to consider a smaller margin area, path width impact, and UKC(Under Keel Clearance) impact and may be affected by specific traffic rules [45]. It has also been reported that this area's voyage planning, monitoring, and navigation habits are different [46, 47]. Therefore, there is a need to construct and validate a model that predicts collision avoidance directions by reflecting figures from collision avoidance algorithms based on human-performed navigation data outside of port-limit from a different perspective.

Second, modeling the outcome of the navigator's perception of the encounter situation after detecting the collision risk. The decision flow of the navigator regarding collision avoidance was identified. It is reported that the navigator's decisions are subjective and contain errors. Interesting contributions have also been reported to compensate for errors and thus contribute to safe navigation. The goal is to develop a decision system for collision avoidance that reduces errors. However, some problems have identified an issue in which varying numerical values are utilized in constructing the decision systems outlined in each respective study. Therefore, the need to build and validate a predictive model of the outcome of the navigator's perception of the encounter situation in the context of detecting the risk of a collision has been found.

1.3 Structure of this dissertation

The scope of this research is limited to the following four works: 1) Acquisition and processing of data required for building a prediction model, 2) Building a prediction model by machine learning, 3) Acquisition of the model, 4) Performance verification of the model, and 5) Proposal of an optimized model.

I. Modeling the ship's collision avoidance direction, which humans operated in an encounter situation.

II. Modeling the ship's encounter situation awareness result

This dissertation consists of four chapters. Chapter 1 presents the necessity of inventing a model that quantifies human behavior outcomes and efforts to perform collision avoidance. In addition, the purpose of this dissertation was presented. Chapter 2 outlines a procedure for determining the parameters of the two vessels, OS and TS. Chapters 3 and 4 consist of the primary studies conducted in this dissertation. The research subjects mentioned in Section 1.2 will be explained on in Chapters 3 and 4, respectively. Chapter 5 summarizes the conclusions obtained in each chapter as a summary of this dissertation and presents the overall conclusions. The structural overview of this dissertation is shown in Figure 1.3.

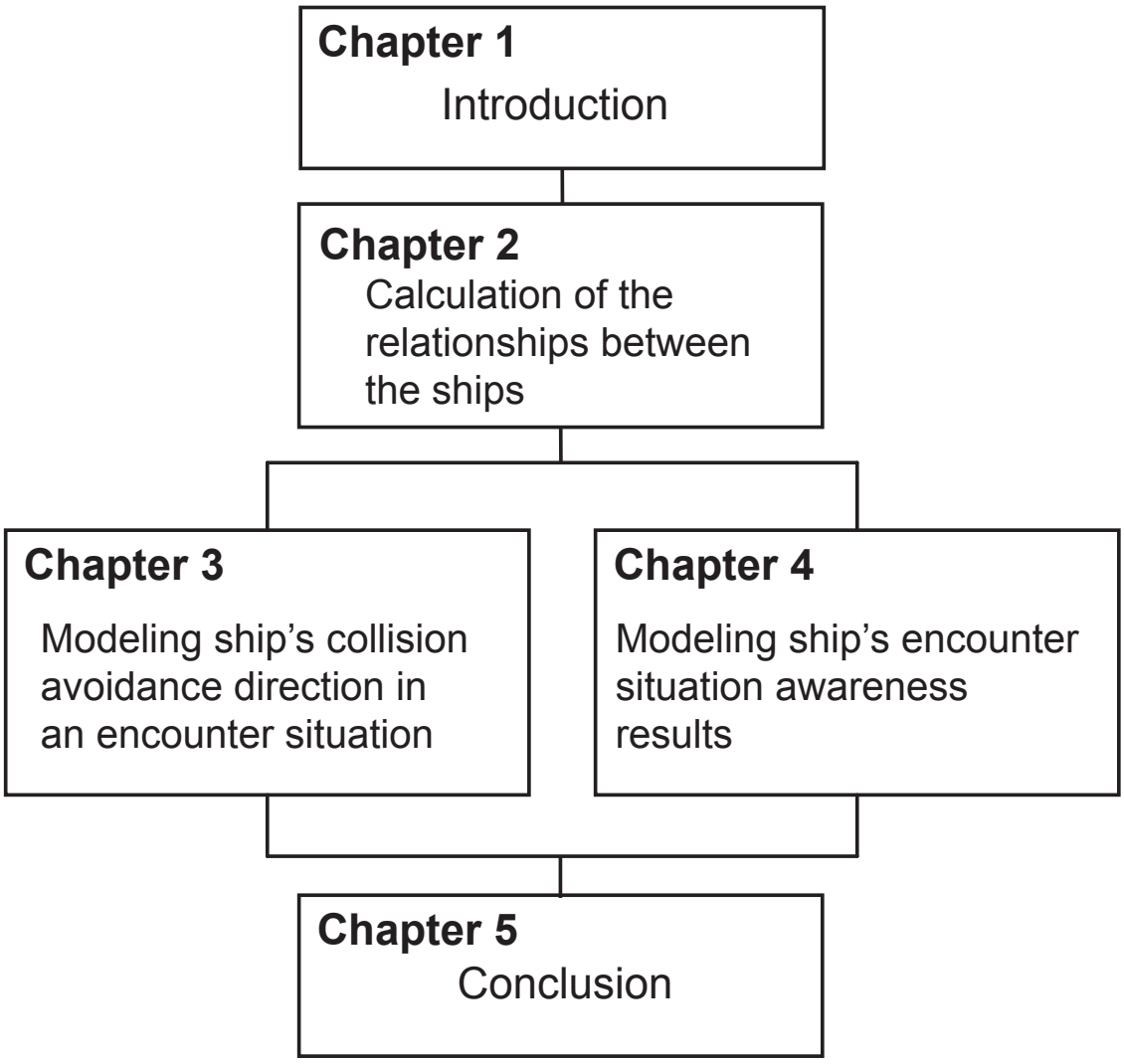

Figure 1.3. Structural overview of dissertation.

Chapter 2

Calculation of the relationship between the ships

This section describes a method of calculating the variables between OS and TS. That is described to define the parameters encountered in the collision situation, which is required for data processing in Chapters 3 and 4.

Figure 2.1 shows the variables of the two ships encountered in a collision risk situation. It is assumed that two ships are on the Earth-fixed coordinate system. Here, the position of the ownship(OS) is $P_o(x_o, y_o)$, velocity is V_o, the course is ψ_o, and the position of the target ship(TS) is $P_t(x_t, y_t)$, velocity is V_t, the course is ψ_t. A_z is the azimuth of TS's position from OS. When OS navigates in its course ψ_o, its relative velocity components on the X and Y axis(ΔX, ΔY), respectively, and its relationship is calculated as follows [48].

$$\begin{aligned} \Delta Y &= V_t \sin\psi_t - V_o \sin\psi_o \\ \Delta X &= V_t \cos\psi_t - V_o \cos\psi_o \end{aligned} \tag{2.1}$$

$$V_r = \sqrt{\Delta X^2 + \Delta Y^2} \tag{2.2}$$

$$\psi_r = \arctan\frac{\Delta Y}{\Delta X} \tag{2.3}$$

Here, V_r is the relative velocity and ψ_r is relative bearing.

When knowing the three parameters (OS's coordinates converted into radians (φ_o, λ_o), distance to the TS (d), and bearing to the TS (Az)), the coordinates of the TS (φ_t,

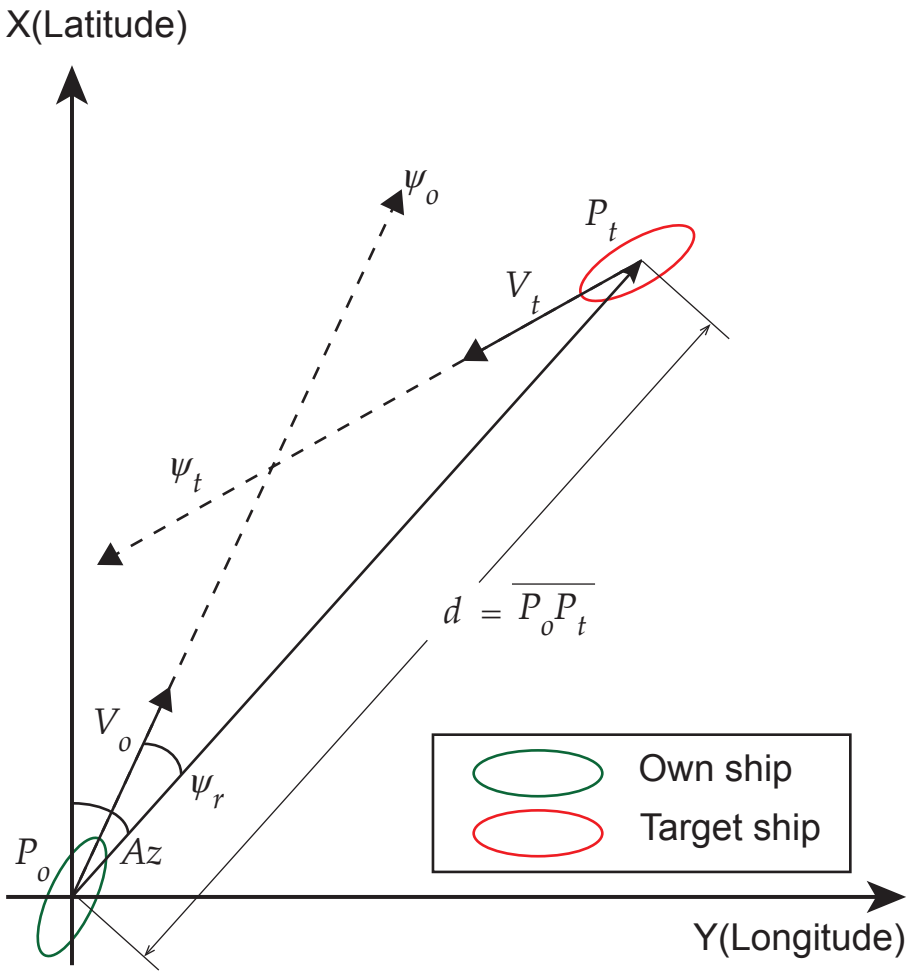

Figure 2.1. Representation of the OS and TS parameters within the earth fixed coordinate system.

λ_t) were obtained using rhumb line calculation [49, 50]. The equation for converting the latitude of the TS into radians (φ_t) is denoted as Equation 2.5, where the angular distance (ϕ) is calculated from Equation 2.4 [49, 50].

$$\phi = d/R \tag{2.4}$$

Here, R is the radius of the Earth (3440 nautical miles).

$$\varphi_t = \varphi_o + \phi \cdot \cos Az \tag{2.5}$$

The longitude of the TS expressed in radians (λ_t) is calculated by adding the dif-

ference in longitude between them ($\Delta\lambda$)(Equation 2.9). The calculation of $\Delta\lambda$ uses the projected latitude difference described in Equations 2.6 and 2.7. The constant δ of Equation 2.6 is derived using the inverse gudermannian function, which provides the elevation of the Mercator projection corresponding to a specific latitude.

$$\delta = \ln(\tan(\pi/4 + \varphi_t/2)/\tan(\pi/4 + \varphi_o/2)) \tag{2.6}$$

As for the projected latitude difference (q), distinct values were employed in cases where a difference in latitude existed, as opposed to cases where no such difference was present, utilizing the constant δ. For the computerized calculation, $10e^{-12}$ was used as a number which is close to zero.

$$q = \begin{cases} (\varphi_t - \varphi_o)/\delta, & \text{If } \delta > 10e^{-12} \\ \cos\varphi_o, & \text{Else} \end{cases} \tag{2.7}$$

$$\Delta\lambda = \phi \cdot \sin(Az/q) \tag{2.8}$$

$$\lambda_t = \lambda_o + \Delta\lambda \tag{2.9}$$

By the way, When knowing the two ships positions, the distance (d) between OS and TS in Equation 2.11 is calculated using rhumb line calculation as follows [49, 50]. The distance calculated in Equation 2.11 is derived from Pythagorean theorem. However, there is a need to correct the projected latitude difference(q)(Equation 2.7) for the correction of the Mercator calculation, which converts the curve to a straight line. $\Delta\lambda$ is the difference in longitude, and a different value is used according to Equation 2.10, because the difference in longitudes between the two positions must be calculated for a close direction.

$$\Delta\lambda = \begin{cases} -(2\pi - (\lambda_t - \lambda_o)), & \text{If } (\lambda_t - \lambda_o) > \pi \\ 2\pi + (\lambda_t - \lambda_o), & \text{If } (\lambda_t - \lambda_o) < -\pi \end{cases} \tag{2.10}$$

$$d = \sqrt{(\varphi_t - \varphi_o)^2 + q^2 \cdot \Delta\lambda^2} \cdot R \tag{2.11}$$

where φ and λ are the values obtained by converting latitude and longitude into radians, respectively, and R has a radius of The Earth (3440 nautical miles).

Using this variable, the DCPA and TCPA, which are used as criteria for determining when a navigator performs a collision avoidance operation, are obtained using Equation 2.12 and 2.13

$$\text{DCPA} = d \times |\sin(\psi_r - Az + \pi)| \tag{2.12}$$

$$\text{TCPA} = d \times \cos(\psi_r - Az + \pi) / V_r \tag{2.13}$$

Chapter 3

Modeling ship's collision avoidance direction in an encounter situation

3.1 Objective of this work

The object of this work is to construct a model that models the direction of avoidance action of the vessel, which is the answer to human behavior in situations where the risk of collision exists. Here, the direction of collision avoidance means only a change of her course. To develop the model, ship trajectory data, which results from actual human behavior, has collected. Based on the collected data, variables that criteria for judgment were obtained when the ship avoided another ship. That contains the basis for the essential judgment used by navigators and the figures obtained from the collision-avoidance algorithm. Subsequently, the performance was verified by constructing an ensemble model that predicted the avoidance direction. The decision-tree-based bagging and the AdaBoost have been used among the models.

Remainder of this chapter is organized as follows. Section 3.2 describes a methodology that includes the establishment and evaluation of an classification model to define collision situations; describes the data, variable construction, and pre-processing used in the work; and describes the relationship between the variables and the direction of the changed course in the event of a collision avoidance action. Section 3.3 presents an analysis of the acquired data and results of the estimated model. Section 3.4 discusses the results.

3.2 Materials and methods

Figure 3.1 shows a flow chart of this study. To illustrate the proposed model, the collision avoidance situation was defined first. It is then described in the order of data acquisition and processing, modeling, and verification methods.

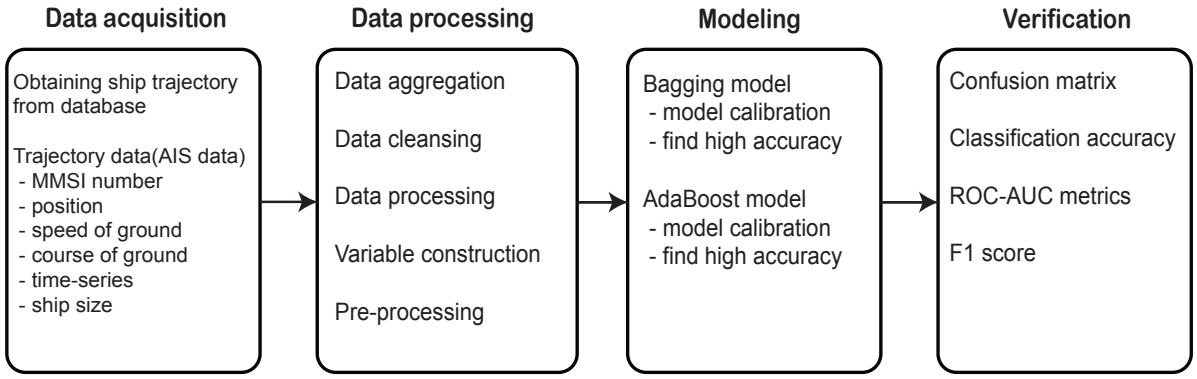

Figure 3.1. Flow charts of model construction and validation.

3.2.1 Collision avoidance

In this subsection, the concept of figures acquired in the collision situation and the collision avoidance algorithm are defined. The encounter situations between the OS and TS are divided into three categories [14]. These are the head-on situation, crossing situation, and overtaking situation. Here, the crossing is divided again into the case where the OS performs a collision avoidance action and the case where TS performs one. Although each situation is distinguished using relative azimuths, DCPA, and TCPA figures, COLREG did not declare clear numerics, and many studies have used different figures to distinguish encounter situations [18, 19, 20, 21, 22]. In this study, encounter situations were classified based on Zhang et al. [21] (See row 4 of Table 1.1).

3.2.1.1 Collision avoidance algorithm

In this study, OZT was used as an algorithm to obtain the predictor variables. The OZT algorithm calculates the area where a ship collision can occur as a line or plane [27, 29]. Various methods for calculating OZT have been proposed. In this study, the OZT calculation model was used to express the area where the course should not be set as a line [48]. This model was calculated based on the safe distance set by the operator. Figure 3.2 (a) illustrates the parameters used to calculate OZT.

The method of geometrically constructing the collision course required for the OZT construction using the parameters described in Figure 3.2 (a) is as follows.

1. Draw a black circle with a safe distance (r_s) as the radius around the positions of OS(x_o, y_o).

2. Draw the tangent lines ($\overline{AA'}$, $\overline{BB'}$) connecting TS and the safety distance circle in step 1.

3. Draw a virtual point C in the opposite direction of the TS's speed and direction vectors (V_t,ψ_t), and draw a purple circle with the speed of the OS(V_o) as the radius around the point C.

4. Obtain the intersection (E, F) of the tangent line($\overline{AA'}$, $\overline{BB'}$)with the speed circle of OS in Step 3, respectively. Here, $\overrightarrow{CE}$and $\overrightarrow{CF}$ are acquired as courses that allow the OS to pass through the TS at a predetermined r_s. When navigating between angles of C_o, TS passes closer than a safe distance set in advance.

The angle α between the tangent lines ($\overline{AA'}$, $\overline{BB'}$) and d is calculated to perform a numerical calculation of the geometrically plotted course ($\overrightarrow{CE}$and $\overrightarrow{CF}$). Hereafter, the course ($\overrightarrow{CE}$and $\overrightarrow{CF}$) is denoted as C_o

$$\alpha = \arcsin(r_s/d) \tag{3.1}$$

where, r_s is a safe distance, which is a hyperparameter of the OZT, and d is the distance between OS and TS.

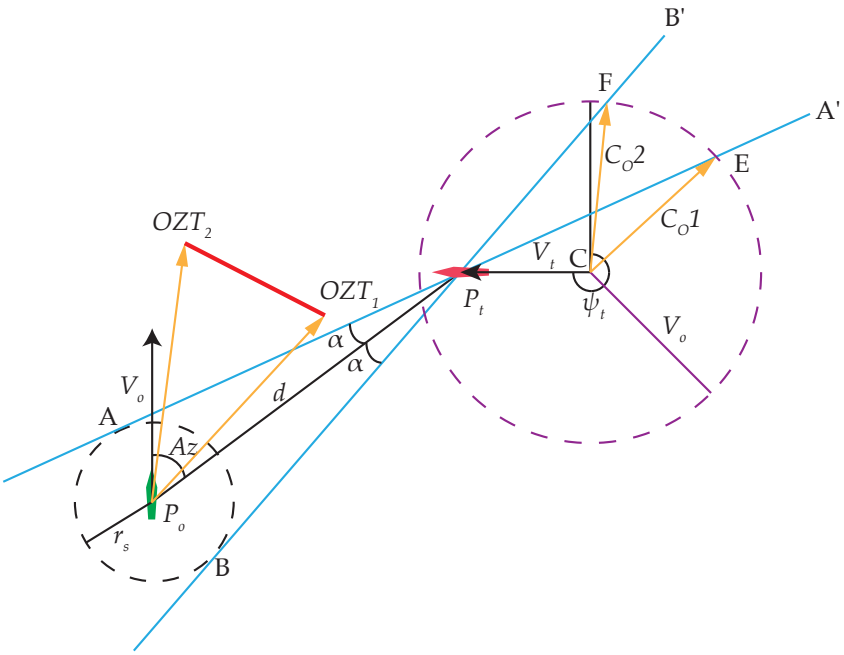

(a)

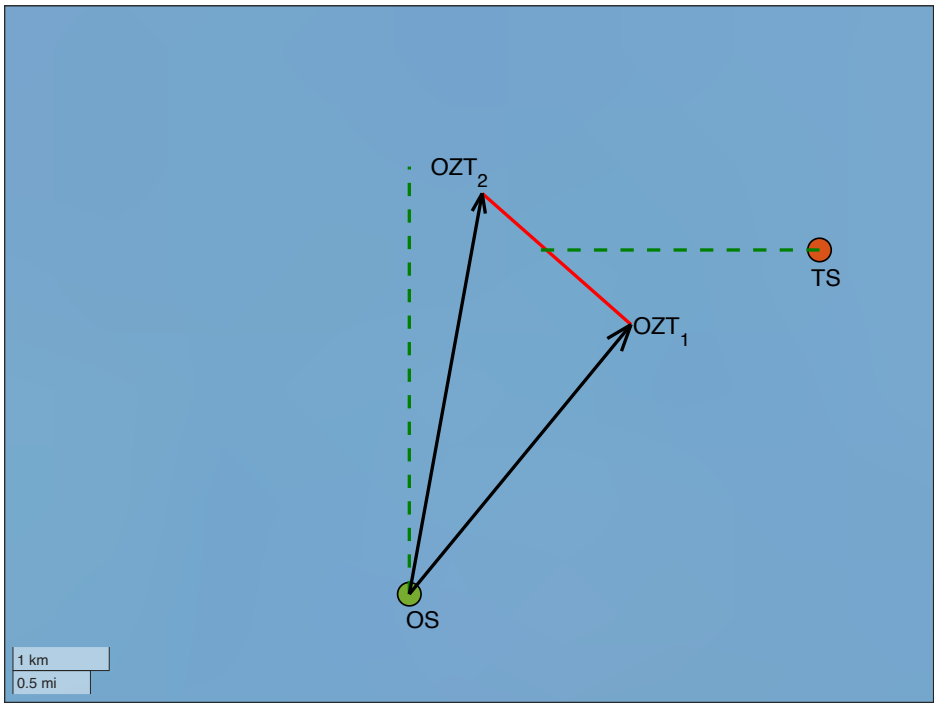

(b)

Figure 3.2. (a) Conceptual diagram of OZT with parameters, **(b)** The computed results of OZT. OS's speed 15 kts, course 000deg, Length Over All 150m. TS's speed 10 kts, course 270deg. *Az* 050deg and the distance of two vessels 3.0 nautical miles.

According to Imazu [48],r_s, a safe distance, was calculated as half the sum of the length of OS and TS, but that was judged as not appropriate. Therefore, the safe distance in this study was set to six times the length of OS, based on the work of Fujii and Tanaka [37]. Take an arbitrary point D by dropping a perpendicular line from point C to the tangent lines respectively. Angles are calculated using the law of sines through the relationship between the divided $\triangle P_t CD$ and $\triangle CDE$ or $\triangle CDF$ [48]. The triangles have a common segment $\overline{CD}$ as shown in Equation 3.2. Equation 3.2 is then organized based on C_o, as shown in Equation 3.3.

$$V_o = \sin(Az \pm \alpha - C_o) = V_t \sin(\psi_t - \pi - (Az \pm \alpha)) = V_t \sin(Az \pm \alpha - \psi_t) \tag{3.2}$$

$$C_o = Az \pm \alpha - \arcsin\left\{ \frac{V_t}{V_o} \sin(Az \pm \alpha - \psi_t) \right\} \tag{3.3}$$

where Az denotes the azimuth of TS from OS, V_t denotes the speed of TS, V_o denotes the speed of OS, and ψ_t denotes the course of TS.

The OZT is constructed by connecting coordinates advanced by the estimated navigation distance ($V_o \cdot TCPA$) from the location of OS (φ_o, λ_o) to the direction of C_o. The coordinates of the OZT are obtained using the Rhumb line calculation [50]. The latitude of OZT (OZT_{Lat}) is calculated as shown in Equation 3.5 using the angular distance (ϕ) calculated from Equation 3.4.

$$\phi = (V_o \cdot TCPA)/R \tag{3.4}$$

$$OZT_{Lat} = \varphi_o + \phi \cdot \cos C_o \tag{3.5}$$

The longitude of the OZT (OZT_{Long}) is obtained by adding the longitude difference ($\Delta\lambda_{OZT}$) between OS and OZT. $\Delta\lambda_{OZT}$ was calculated using the projected latitude difference obtained in Equation 3.6 and Equation 3.7.

$$\delta_{OZT} = \ln(\tan(\pi/4 + OZT_{Lat}/2)/\tan(\pi/4 + \varphi_o/2)) \tag{3.6}$$

$$q = \begin{cases} (OZT_{Lat} - \varphi_o)/\delta_{OZT}, & \text{If } \delta_{OZT} > 10e^{-12} \\ \cos\varphi_o, & \text{Else} \end{cases} \tag{3.7}$$

$$\Delta\lambda_{OZT} = \phi \cdot \sin(C_o/q_{OZT}) \tag{3.8}$$

$$OZT_{Long} = \lambda_o + \Delta\lambda_{OZT} \tag{3.9}$$

where, φ_o and λ_o are figures obtained by converting the latitude and longitude of the OS into radians, respectively, and R is the radius of The Earth (3440 nautical miles).

Figure 3.2 (b) is an example of OZT calculation by above steps.

3.2.2 Data acquisition

In this subsection, the data used in this study is described, including the data collection and adopted processing methods.

3.2.2.1 Data collection

For modeling(Construction and evaluation), variables extracted from the collected data. Among these, followed data has required; the trajectory data take action to avoid risk of collision. Methods for collecting such data include ship maneuvering simulations, traffic surveys, and scenario-based numerical simulations [40].

In the case of ship maneuvering and scenario-based numerical simulations, there is a problem that the actual situation cannot be reflected at sea. However, among the methods of collecting data, the method of collecting AIS(Automatic Identification System) data has the advantage of being able to reflect the actual situation at sea, unlike the previous two methods [51]. AIS data are classified as static information, dynamic information, and navigation-related information [52]. The data were extracted in CSV format from the AIS database constructed on the Advanced Navigation System of the Tokyo University of Marine Science and Technology. The extraction range of data is latitude 34°30.0′ N $\sim$ 35°01.8′ N and longitude 139°12.6′E $\sim$ 139°39.6′E. The reason for using only the data in the above boundary is to exclude data affected by traffic rules in Tokyo Bay. Although the area contains an island and the recommended route, the area has the relative meaning of the open waters outside the port limit. In addition, no collision avoidance action near the recommended route was detected. The period of extraction was continuous 24-h data from January 1, 2017, to December 31, 2019. Figure 3.3 illustrate the sea areas in which data were collected.

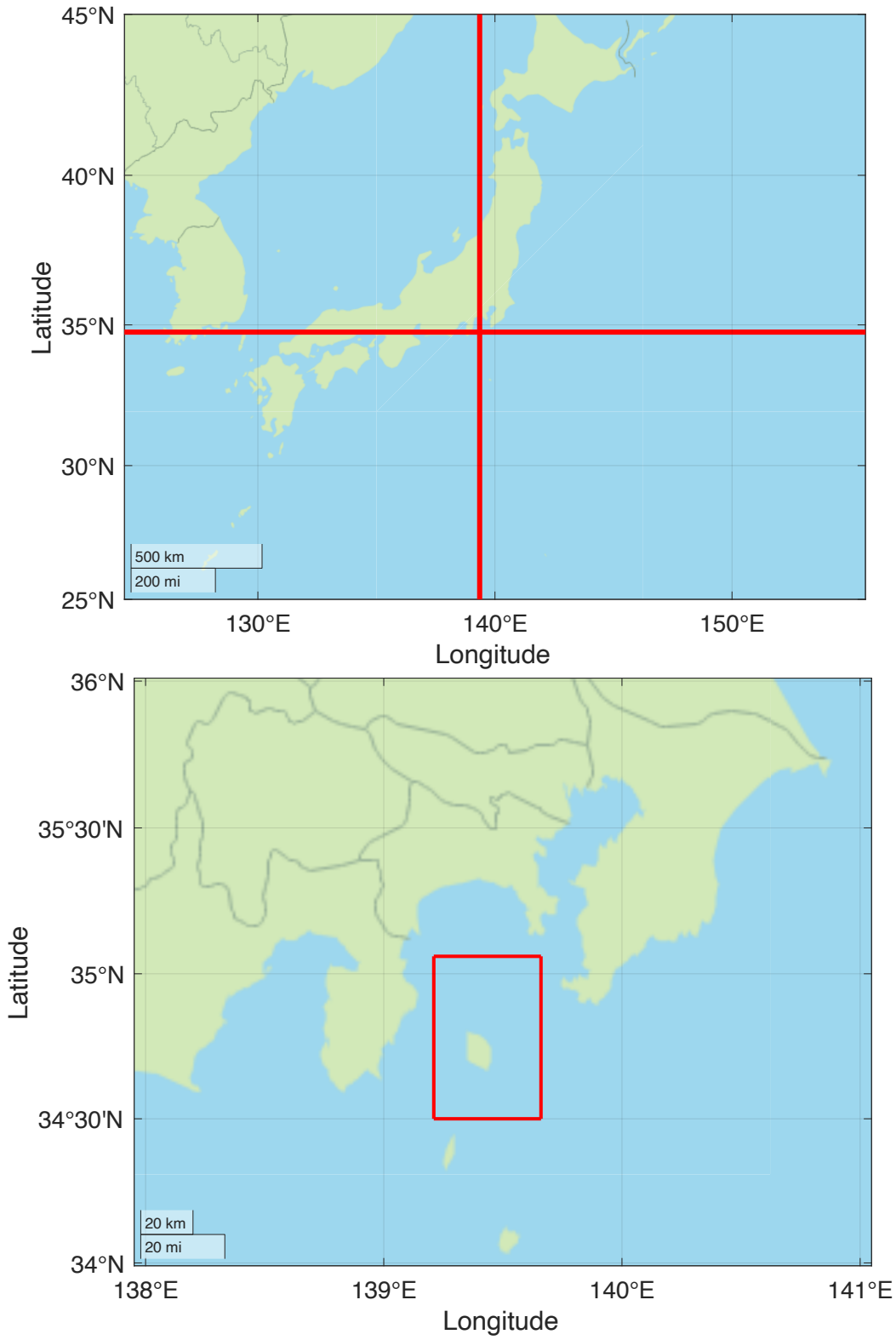

Figure 3.3. Geographical visualization of the data collected area (Near Oshima, Japan).

3.2.2.2 Data processing

The collected data were processed in four steps, and Figure 3.4 illustrates the flow of the processing procedures.

- **Step 1** : (Data aggregation and cleansing): The data required for the experiment were extracted from the raw data (static and dynamic information of AIS data). When the extraction was performed, the static information(ship's size and MMSI) were extracted, and the dynamic information (MMSI, coordinate (latitude, longitude), ship's speed, and course, and time-series) were extrated. This information was aggregated based on the MMSI number. Subsequently, missing values were removed from the aggregated information, and only the data in the extraction range described in Section 3.2.2.1. were preserved. Among these, day data with a Beaufort scale of 7 or higher were excluded to minimize weather impacts [53]. Finally, the data of each ship were stored in an independent file based on the MMSI number.

- **Step 2** : (Data interpolation and resampling): The data required to obtain predictor variables should be compared based on the same time interval. This is because collision avoidance is a consequence of simultaneous operation with a risk of collision. Unfortunately, AIS data are stored irregularly according to standards [54]. Therefore, interpolating the data was necessary. When interpolating data, linear interpolation was performed if the time-step interval of the data points was 60 s or less, and cubic spline interpolation was performed if the time-step interval was between 60 s and 180 s. If it exceeds 180 s, there is a concern that data that do not exist may be excessively interpolated, so it was not interpolated. The interpolated data were re-sampled at intervals of 30 s.

- **Step 3** : (Data processing according to logic): The data of each ship stored in the process of Step 2 were called using a double loop. The double loop was derived using the total number of files (a count of ships detected). The vessel called in the first loop is named OS, and that in the second loop is named TS. Then, check whether the two data sets overlap in time series and traffic within a certain distance. Collision avoidance occurs because the two ships interact within the same space and time. According to the ship domain theory, if the minimum passage distance between the OS and TS is less than six times length of the OS, it is excluded from the data for variable construction. The reason is to exclude data that pass through dangerous distances.

Step 3.1, Identification of the point of altering the course : To obtain data on which the vessel has performed altering her course, t_{alter} which the time the vessel began to change her course must be identified. The commencement of the alteration was identified using the curvature(k). The curvature was calculated by numerically differentiating the set of trajectory coordinates $P = \left\{ P = \left(P_x, P_y \right) \mid P_1, P_2, ..., P_n \right\}$ of the ship operated in the Earth coordinate system, with longitude as the x-axis and latitude as the y-axis. Thereafter, the time at which the curvature reached its maximum value was identified as t_{alter}.

- **Condition 1**: It was confirmed that the time series data of OS and TS were preserved for 1 hour before and after based on the point at which the minimum passage distance between the two ships occurred (d_{min}). The OS and TS data were re-sampled for 30 s in step 2. If the number of data points was less than 120, the data were not intact. Hence, they were excluded from the training data.

- **Condition 2**: At the time of t_{alter}, it was confirmed that altering course operation performed by the OS was owing to the risk of collision. When interference by the OZT occurred in front of the OS's course at times of t_{alter}, the manoeuver was considered a collision avoidance operation.

- **Condition 3**: It was confirmed whether OS was in a give-away situation(including both head-on and crossing give-away).

$$k = \left(\left| \ddot{P}_x \cdot P_y - \dot{P}_x \cdot \ddot{P}_y \right| \Big/ \left| \dot{P}_x \cdot \dot{P}_x + \dot{P}_y \cdot \dot{P}_y \right| \right)^{1.5} \tag{3.10}$$

Step 3.2, Identification of single avoidance situation : In the algorithm of Step 3, data that performed the collision avoidance operation was stored as the index of OS. The variable was constructed by extracting from the data only when the OS performed a single operation with TS.

Step 3.3, Variable construction : The predictive variable was constructed using the indicators that the ship operator determines the risk of collision and the variables obtained by the collision avoidance algorithm. The variable was calculated from the time of t_{alter}. In addition to the DCPA and TCPA indicators used in ARPA RADAR, the length ratio of two ships, the speed ratio of two vessels, and the Aspect which is the relative bearing calculated by the sight of the TS were selected as

predictor variables. In addition, the relative direction (θ_{OZT}) and distance (d_{OZT}) to OZT, which enable passage from the safe distance set by the operator, were selected as predictors. Here, θ_{OZT} and d_{OZT} obtained the values of C_o with a small difference in angle based on the course of the OS. Moreover, the variables corresponding to the angle were converted from -180° to 180° by relative bearing based on the course of the OS. Additionally, the response variable was used as a categorical variable. If the direction in which the course changes to avoid a collision with the target ship is in the starboard direction, it is 1; otherwise, it is 0.

- **Step 4** : (Data Pre-processing): The pre-processed data were converted to be suitable for model construction. This is important because it affects the performance of the model [55]). Since the predictor used in this study was a continuous variable, it was standardized to unify the scale. In addition, data points were uniformly sampled through under-sized sampling to prevent the model from degrading predictive power due to an imbalance in the resulting variables.

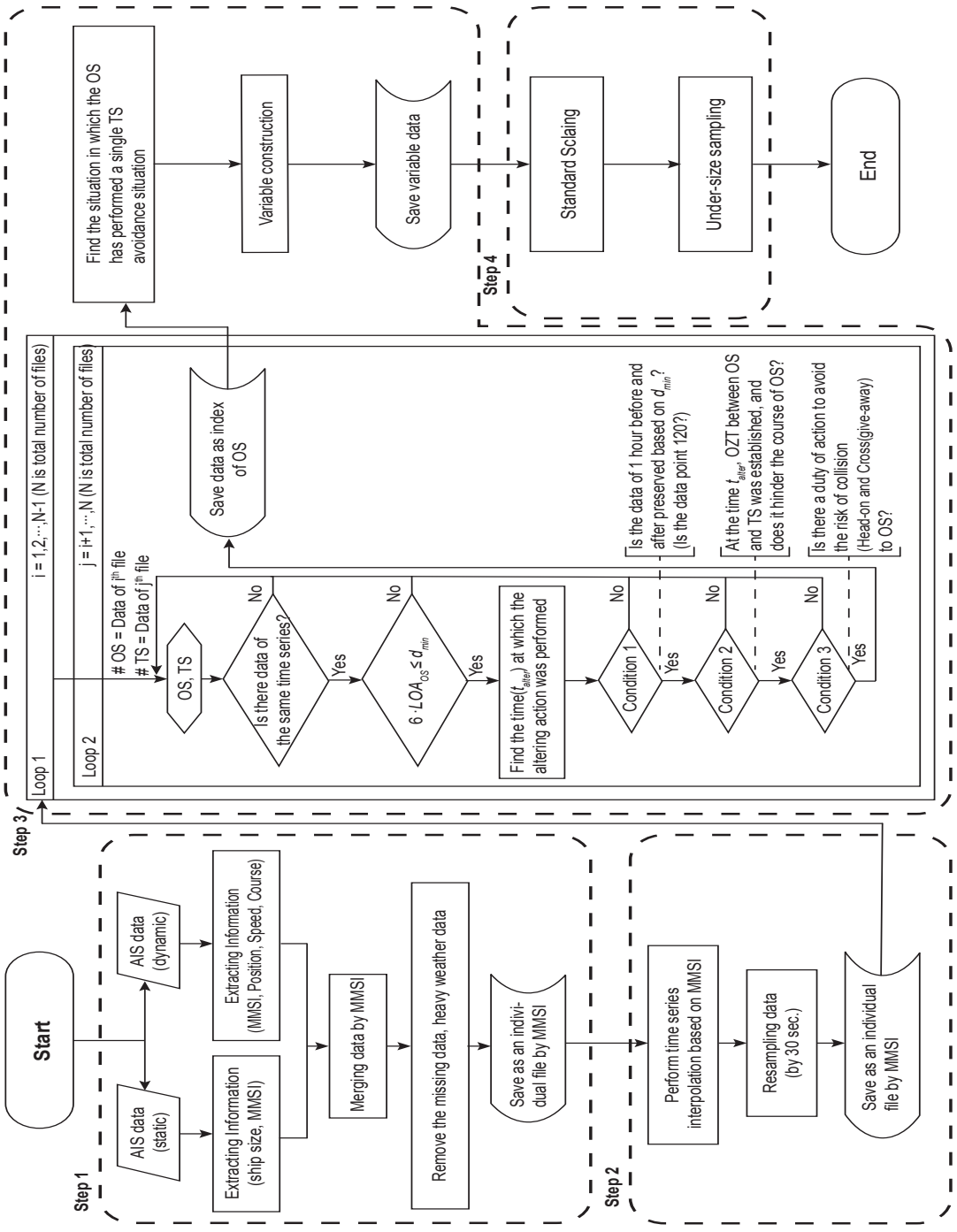

Figure 3.4. Flow chart of data processing and variable construction.

3.2.3 Ensemble model

An ensemble classification model is formulated to estimate the relationship between the obtained predictor variables and the direction of course change, which is the result of collision avoidance. Figure 3.5 illustrates a framework in which the variables calculated using the acquired data were used to train an ensemble model. The inputs were the variables obtained through the process described in Section 3.2.2.2. Furthermore, the output was the direction of collision avoidance predicted using the trained model. To clarify the framework, the base model used in the ensemble model is described, followed by the Bagging, AdaBoost, and hyperparameters. Ultimately, the model's validation method is delineated.

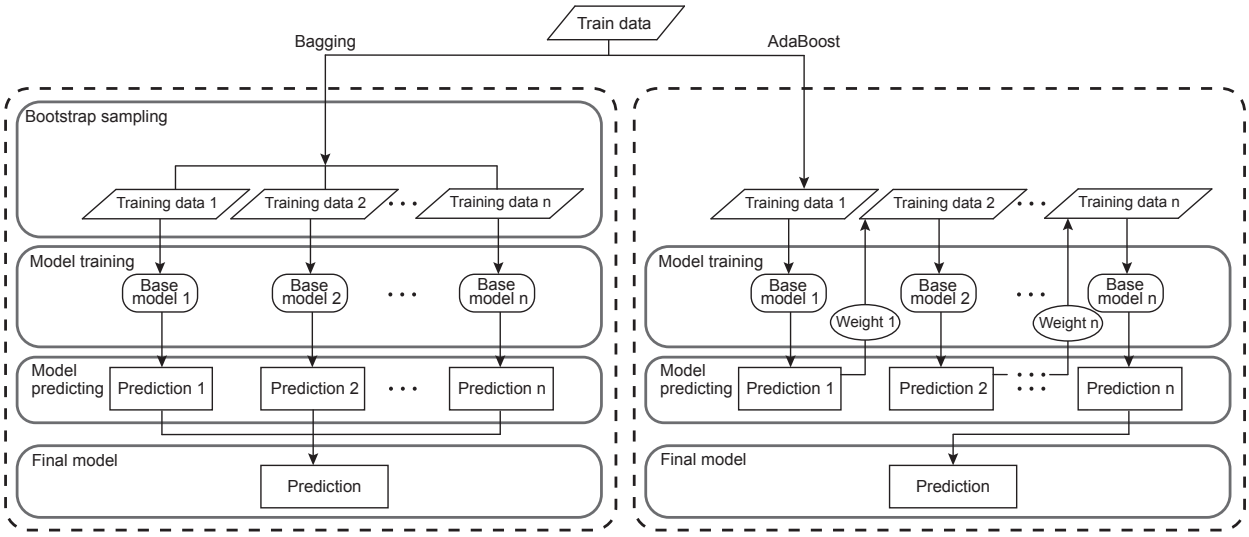

Figure 3.5. Illustration of model framework for Bagging (Left), and AdaBoost(Right).

3.2.3.1 Base model

Ensemble models are a supervised learning algorithms that combines multiple base models for improved predictive capabilities [56]. A Decision-tree model was used as the base model for the ensemble model. Because this model can be constructed efficiently even for massive amounts of data, the premise for the data distribution is not required [57]. While various decision-tree models exist, I opted to utilize the widely employed Classification And Regression Trees (CART) model for analysis. The Decision-tree model divides the space such that data points with the same result variable are grouped while dividing the nodes. When dividing a node in the CART model, the Gini index, which is a measure of the impurity of data, was used as a reference. This is the sum of the product of probability (p_i) that belongs to the class (i) of the outcome variable among the number of M result variables when divided between a node (S) and the probability that it does not belong.

$$G(s) = \sum_{m=1}^{M} p_i(1 - p_i) \tag{3.11}$$

3.2.3.2 Bagging and AdaBoost model

The Bagging model is an ensemble model that is based on a decision tree. The advantage of the Bagging model is that it is robust to data noise of the data and the possibility of low overfitting [56, 58]. In addition, each model was independent, because the base model was constructed in parallel. K pieces of training datasets were extracted by sampling using the replacement method, and K pieces of bootstrap samples were constructed and used as a training dataset [59]. Subsequently, the base models were created using multiple datasets and combined to build a final model. The final model is derived by combining the results of the multiple-base model. The final model is formulated as follows [59, 60].

$$C^*(x) = \text{argmax}_y \left(\sum_{i=1}^{K} I(f^{(i)}(x) = y), y \in \{0, 1\} \right) \tag{3.12}$$

where, $C^*(x)$ is the final model, I is the indicator function, $f^{(i)}(x)$ is the prediction model for the reconstructed and extracted bootstrap samples, and y is the outcome variable.

The AdaBoost model improves classification performance by constructing a strong learner by linearly combining the learning outcomes of weak learners based on decision trees [61]. Moreover, it is known for its excellent performance in simple implementation and generalization [62]. Starting with the first iteration, the weak learner learns and delivers the classification result information to the next classifier. The following classifiers leverage the information received from existing classifiers to improve the weight of the data that fail to be classified. That is, the misclassification rate is lowered while the weight of the sample misclassified by the previous classifier is changed. The model is formulated as follows [60, 61].

$$C^*(x) = \text{sign} \left[\sum_{j=1}^{M} a_j h_j(x) \right] \tag{3.13}$$

where, $C^*(x)$ is the final model, a is the weight, h is the weak learner, and N is the number of repetitions.

3.2.3.3 Hyperparameters and model assessment

The ensemble models used in this study are the Bagging and AdaBoost models based on the Decision Tree. Each model adjusts the hyperparameters to find the optimal prediction.

Hyperparameters of the Decision Tree model: The depth of the tree was adjusted to prevent overfitting. Because the Decision Tree model can cause overfitting by expanding trees to minimize impurities. Depth was adjusted to max (non-limited), 1, 3, 5, and 7 when applied to the bagging tree, and 1, 3, 5, 7, and 9 when applied to AdaBoost.

Hyperparameters of the Bagging model: The sampling rate determining the number of base models and the ratio of bootstrap samples was adjusted. The base models were 10, 30, 100, 500, and 1000, and the sampling rates were 0.1, 0.3, 0.5, 0.7, and 1.0.

Hyperparameters of the AdaBoost model: The number of the base model and learning rate were adjusted. The base models were 10, 30, 100, 500, and 1000, and the learning rates were 0.0001, 0.001, 0.01, 0.1, and 1.0.

Grid search: To perform training reflecting all hyperparameters, model learning of all cases must be performed. Grid search was performed for efficient model training. Grid Search uses predetermined figures of hyperparameter candidates to derive an optimal hyperparameter after cross-validation for all cases. Here, Test data should not be involved in Grid search. Therefore, the set of variables was split into Train-validation data and Test data, and the Train-validation data was split into Train data and Validation data set once again. After that, Grid search was performed using Train data and Validation data set to obtain hyperparameters with high acuity. Finally, the model was trained using hyperparameters and train-validation data obtained through grid search

The performance of the ensemble classification model was assessed using the confusion matrix and ROC-AUC metrics. Accuracy, precision, recall and F1-score were also used for the performance evaluation. These measures are derived from the calculation of a confusion matrix [63]. The matrix represents the anticipated values of the labels derived from the actual labels. Figure 3.6 illustrates the confusion matrix for binary classification. Confusion matrix is the basis for calculating metrics that

measure the performance of a classification model. The terms of the confusion matrix are summarized below.

TP (True Positive): This is the case, the model predicts True and the actual answer is True.

TN (True Negative): This is the case, the model predicts False and the actual answer is False.

FP (False Positive): This is the case, the model predicts True and the actual answer is False.

FN (False Negative): This is the case, the model predicts False and the actual answer is True.

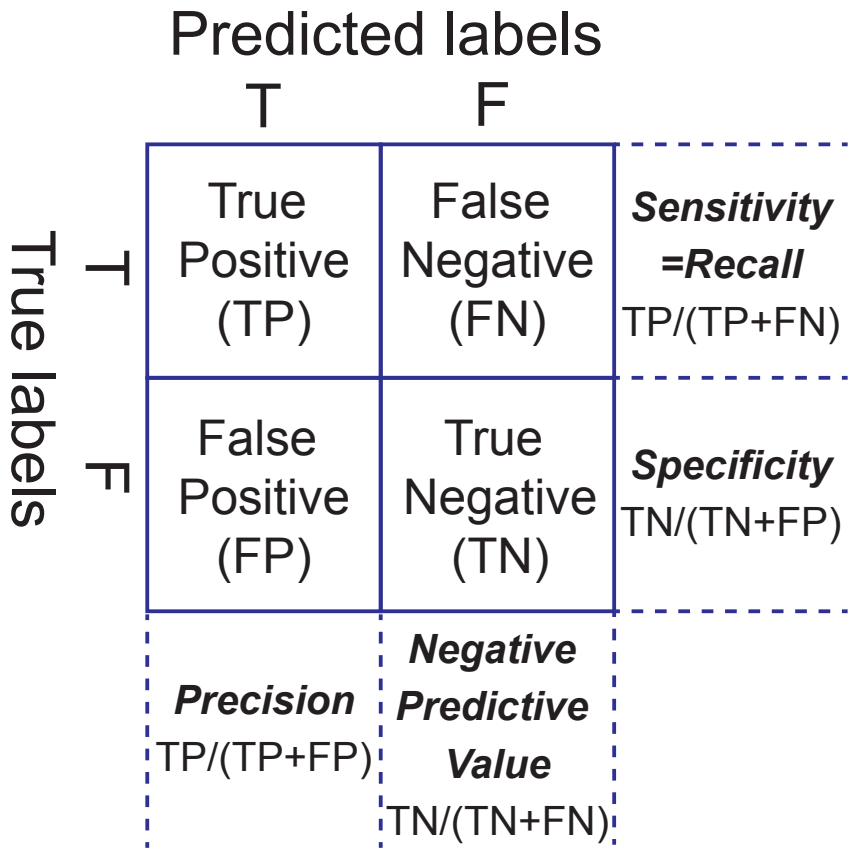

Figure 3.6. Illustration of confusion matrix for binary classification.

The model's accuracy is the rate at which it correctly predicts the answers. However, when the data is imbalanced, using only accuracy may not accurately assess the model. Therefore, recall and precision have to be used to evaluate whether the classification was done correctly. Accuracy is calculated by Equation 3.14.

$$\text{Accuracy} = \frac{\text{TP} + \text{TN}}{\text{TP} + \text{TN} + \text{FP} + \text{FN}} \tag{3.14}$$

Precision is defined as the likelihood that the true label is positive given a positive prediction, and does not ensure the model's accuracy for negative predictions. Precision is calculated by Equation 3.15.

$$\text{Precision} = \frac{\text{TP}}{\text{TP} + \text{FP}} \tag{3.15}$$

Conversely, recall represents the probability of a positive prediction given a positive true label, and does not offer insights into predictions for negative true labels. Recall is calculated by Equation 3.16.

$$\text{Recall} = \frac{\text{TP}}{\text{TP} + \text{FN}} \tag{3.16}$$

The F1 score, an evaluation metric that considers both recall and precision, is calculated using Equation 3.17. Recall and Precision, as previously reported, are complementary evaluation metrics, thus they are utilized together in the integrated metric, F1 score. F1 score takes into account both Precision and Recall, giving a high value when both are high without being skewed.

$$\text{F1 score} = \frac{2 \times \text{Precision} \times \text{Recall}}{\text{Precision + Recall}} \tag{3.17}$$

The receiver operating characteristic (ROC) curve is a performance metric derived from the combination of the true positive rate (TPR) and the false positive rate (FPR). The TPR is equivalent to the recall and sensitivity, while the FPR is computed as 1 minus the specificity. Specificity represents the likelihood of a negative prediction when the true label is negative. Unlike the recall, the FPR does not offer insights into predictions made when the true label is positive. The area under the curve (AUC) is

depicted by plotting the TPR on the y-axis and the FPR on the x-axis, as indicated in Equation 3.18. And FPR is calculated by Equation 3.19.

$$\text{AUC} = \int_0^1 \text{TPR}(\text{FPR}^{-1}(x))dx \tag{3.18}$$

$$\text{FPR} = \frac{\text{FP}}{\text{FP + TN}} \tag{3.19}$$

Python and its libraries have been used as tools for model construction and evaluation [64, 65, 66, 67].

3.3 Result

3.3.1 Result of data analysis

Through AIS data acquisition and pre-processing, the predictive variables and response variables used in the model construction were obtained. Seven continuous variables were used here. As a result of the data pre-processing, 950 pieces of data were obtained. However, the variable was biased when altering the course to the starboard side (starboard 629, port 321). Since this result affects the model's learning and predictive power, it was balanced to 483 data points by undersize sampling (starboard 284, port 199).

Table 3.1 briefly describes the characteristics and statistics of variables extracted from the data. Figure 3.7 shows the distribution of the predictor set. Most data were collected when the speed ratio of the OS and TS was around 1, that is, the speed was similar. Evidently, a sample of vessels less than twice the size of OS was collected more than vessels more than twice the length of OS. Most of the collected samples can be found to perform the collision avoidance action at a time point of 30 min or less of TCPA. However, the aspect, which is a characteristic of the relative bearing looking at the OS from TS, had a high level of around 000°. A large number of samples were collected where the ship was positioned in the direction of the other ship's positive bow at the time the ship carried out its evasive maneuver.

Table 3.1. Description of data and statistical metrics.

Variable	Type	Unit	Count	Mean	Std	Min	Max
Speed rate	Continuous	-	483	1.06	0.40	0.30	2.50
Size rate	Continuous	-	483	1.26	0.84	0.20	4.90
DCPA	Continuous	Nautical mile	483	0.60	0.51	0.00	4.40
TCPA	Continuous	Hour	483	0.39	0.12	0.06	0.76
Aspect	Continuous	Degree	483	-4.39	44.94	-179.90	178.90
d_{OZT}	Continuous	Nautical mile	483	5.31	1.98	0.00	11.50
θ_{OZT}	Continuous	Degree	483	-2.47	12.24	-52.21	57.32
Y	Categorical	-	483	-	-	-	-

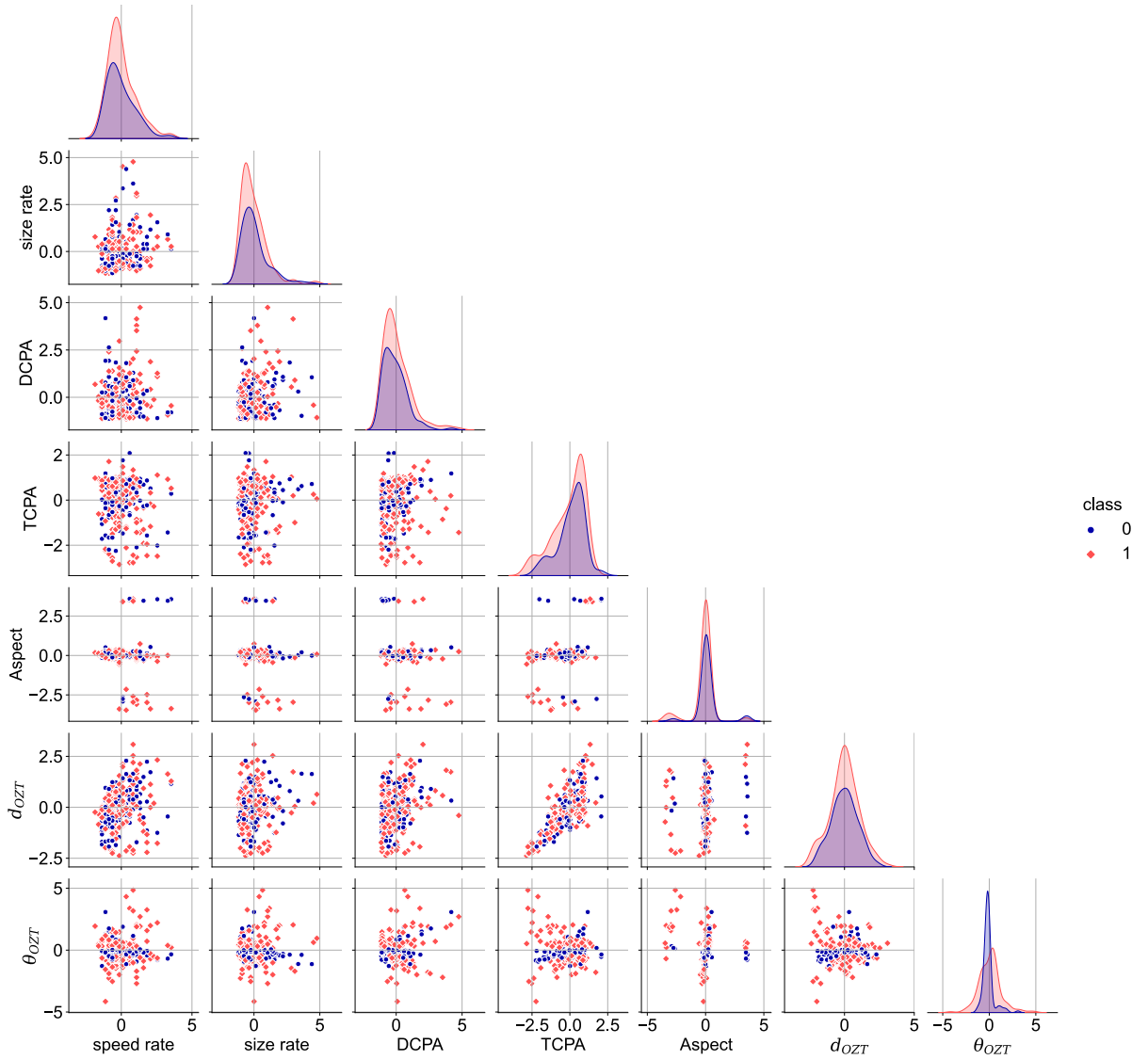

Figure 3.7. Distribution of the predictor variables. Classes 0 and 1 denote altering course to port and starboard sides, respectively.

Table 3.2 shows the correlation matrix between variables. There was the strongest positive correlation between TCPA and the distance to OZT.

Table 3.2. Correlation matrix between predictor variables.

	Speed rate	Size rate	DCPA	TCPA	Aspect	d_{OZT}	θ_{OZT}
Speed rate	1						
Size rate	0.25	1					
DCPA	0.01	0.16	1				
TCPA	-0.05	-0.03	0.07	1			
Aspect	-0.05	-0.10	-0.13	0.25	1		
d_{OZT}	0.33	0.10	0.26	0.74	0.13	1	
θ_{OZT}	0.09	0.04	-0.11	-0.05	-0.13	0.00	1

3.3.2 Result of model construction

The classification model was constructed using the ensemble classification. In this section, the results of the model's construction are first described, and then the verification results are reported.

3.3.2.1 Construction result

Each classification model was a decision-tree-based model trained by adjusting the hyperparameters. Hyperparameters were explored based on good accuracy and prevention of excessive learning. The hyperparameters adjusted were the number of classifiers, sample rate, and branch depth for the Bagging model and the number of classifiers, learning rate, and branch depth for the AdaBoost model. Cross-validation was performed to prevent overfitting in the learning. The Bagging model (depth 1) exhibited the lowest accuracy, with a value of 0.793. The Bagging models with depth Max and 7 achieved an accuracy of 0.917. The AdaBoost model with a depth of three obtained high accuracy(0.934). In terms of F1-Score, which takes into account recall and bias, the Bagging (depth Max and 7: 0.930) and AdaBoost (depth 3: 0.944) models were also acquired as the highest-performing models.(See Table 3.3)

Table 3.3. Estimation of the optimal hyperparameters for models.

Model	Feature	NoE	$Rate_s$	$Rate_l$	Acc.	Precision	Recall	F1-score
Bagging	Max	100	1.0	-	0.917	0.917	0.943	0.930
	1	1000	0.1	-	0.793	0.881	0.743	0.806
	3	10	1.0	-	0.909	0.904	0.943	0.923
	5	100	0.7	-	0.901	0.903	0.929	0.915
	7	500	1.0	-	0.917	0.917	0.943	0.930
AdaBoost	1	10	-	0.0001	0.868	0.865	0.914	0.889
	3	1000	-	1.0	0.934	0.931	0.957	0.944
	5	500	-	1.0	0.917	0.917	0.943	0.930
	7	30	-	1.0	0.868	0.865	0.914	0.889
	9	10	-	0.0001	0.868	0.865	0.914	0.889

where Feature is the depth of base model, NoE is the number of base model, $Rate_s$ the sampling rate, $Rate_l$ is the learning rate, and Acc. is Accuracy.

3.3.2.2 Validation result

The confusion matrix for the models is shown in Table 3.4. Furthermore, the ROC-AUC metrics were computed, and ROC curves were generated (Figure 3.8). AUC scores of models except AdaBoost models (depth1, 7, 9) were obtained at 0.9 or higher. The model that obtained high accuracy in the Bagging was the model (depth max, 7). After that, the model (depth 3) showed high accuracy. The model (depth Max, 7) acquired a high recall and F1-score. After that, the model (depth 3) showed a high score. Therefore, in the Bagging model, the model (depth Max, 7) appears to be the best, but this model was founded that over-fitted with 1.0 accuracy of training. In the AdaBoost model, the model (depth 3) was obtained with high accuracy, recall, and F1-Score. However, the accuracy of all the training performed through the AdaBoost model was founded to be over-fitted to 1.0. The Bagging model (depth of 3) was not overfitted, with a training result of 0.906, and the validation results showed high accuracy, recall, and F1-score. Therefore, the Bagging model with depth 3 exhibited the best performance among the models compared.

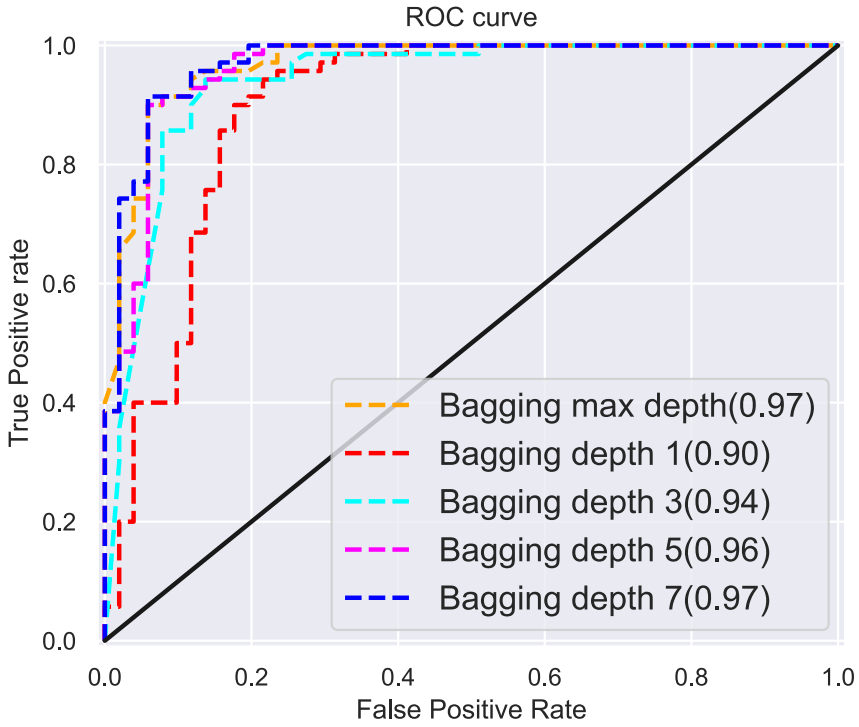

(a)

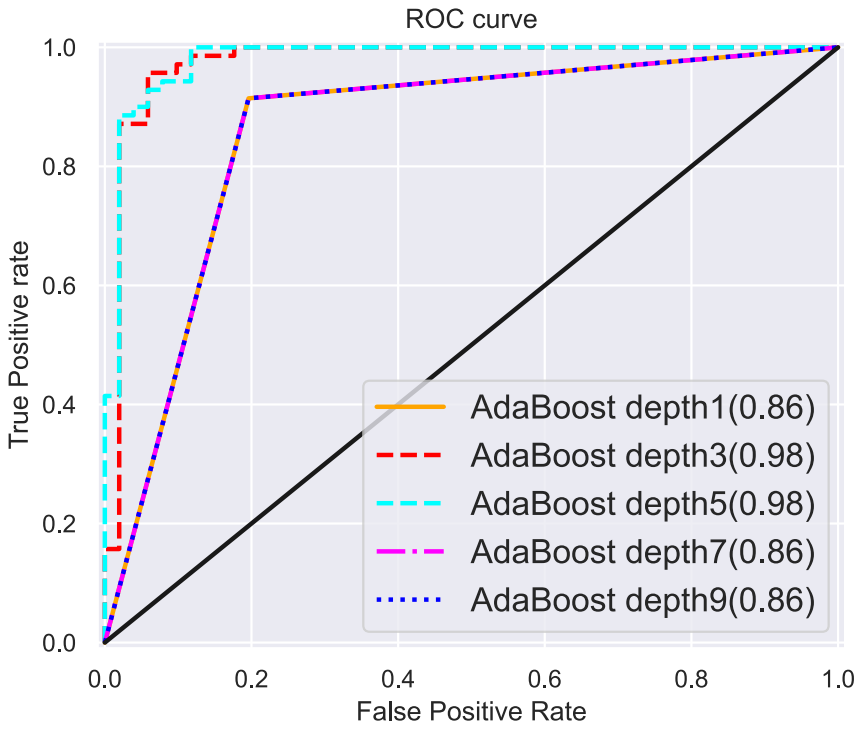

(b)

Figure 3.8. ROC and AUC metrics of Bagging model **(a)** and AdaBoost model **(b)**.

Table 3.4. Confusion matrix for high accuracy models.

Bagging(Max)			Bagging(1)			Bagging(3)			Bagging(5)			Bagging(7)		
True	Predicted		True	Predicted		True	Predicted		True	Predicted		True	Predicted	
	0	1		0	1		0	1		0	1		0	1
0	45	6	0	44	7	0	44	7	0	44	7	0	45	6
1	4	66	1	18	52	1	4	66	1	5	65	1	4	66
AdaBoost(1)			AdaBoost(3)			AdaBoost(5)			AdaBoost(7)			AdaBoost(9)		
True	Predicted		True	Predicted		True	Predicted		True	Predicted		True	Predicted	
	0	1		0	1		0	1		0	1		0	1
0	41	10	0	46	5	0	45	6	0	41	10	0	41	10
1	6	64	1	3	67	1	4	66	1	6	64	1	6	64

Here, 0 and 1 mean altering course to port and starboard, respectively. And Positive label was set as 1.

3.4 Discussion

This work utilized an ensemble classification model to classify the direction of avoidance as determined by the vessel operator. The main contribution of this study was the development of a model to predict the avoidance direction determined by the operator for collision avoidance. In this section, the variables and models used in the study, and the results has discussed.

3.4.1 Discussion of variables and models

As described in section 3.2, seven numerical-type predictor variables were applied to the model: vessel size ratio, speed ratio, DCPA, TCPA, aspect, distance, and heading to the expected hazard (OZT). Seven predictor variables were applied to the model for the following reasons: First, information can be acquired by vessel operators during the information-gathering phase of making avoidance-direction decisions [12, 23, 68]. Second, it reflects the characteristics of the information that humans perceive when making collision-avoidance decisions [69, 70]. Third, The data obtained from OZT means making the model train the relationship between collision avoidance algorithms and human decisions in the model. Furthermore, by providing the

model with figures of the bearing and distance to the region where the collision is expected, it provides a basis for estimating the margin distance humans judge when determining the avoidance maneuver. Variables used in the model are data obtained in a relative relationship with TS around the OS. Moreover, the output is the predicted direction of avoidance of the OS. However, this does not mean predicting only the direction of avoidance of OS. Because the relationship between OS and TS is relative. Therefore, it is possible to estimate the behavior of the TS from the point of view of the OS using the result of this model. For the model constructed in this study to be used to predict the direction of avoidance, a model must be constructed that achieves high performance using data from which the direction of avoidance is determined in a collision-avoidance situation. Ensemble models introduced for model construction have the advantage of being able to combine several base models to create strong models [71]. However, the combination of a single model does not mean performance improvement. In addition, the model's output analysis is complicated [71]. A random forest model was developed to improve the predictive power of the Bagging model and prevent overfitting. The model randomly selects predictor variables to prevent overfitting and finds optimal values [72]. However, this method was not used in our study to use all of the acquired predictor variables. In addition, the boosting models have a characteristic in which the weight of the first model affects the results of the following model [71]. It is also known as a model sensitive to the characteristics of datasets [71]. Therefore, among the boosting models, the simplest and most general AdaBoost model was used. In addition, in this study, Grid search was performed to find optimized parameters. As outlined in Section 3.3.2, the evasive maneuver of a vessel is categorized into two scenarios: when the vessel turns to starboard and when it turns to port. Subsequently, a predictive model to determine the direction of the evasive maneuver was developed. The results mentioned in Section 3.3.2.1 and validated by the confusion matrix with ROC curve and AUC score in Section 3.3.2.2, confirm that an excellent model can be constructed using the model proposed in this study. Despite the rejection of models with solid performance indicators in validation, the models that demonstrated suboptimal outcomes were able to develop. This result is seemed to follow the report that compared to the bagging model, boosting is sensitive to complex, noisy data characteristics, and there is a risk of overfitting [57]. In particular, based on the AUC evaluation criteria of Muller et al. [73], the accuracy and performance of the classifier were inferred to be good because the AUC score of the classifier was obtained at 0.9 or higher.

3.4.2 Discussion of results

By constructing and modeling variables using the acquired data, a model was established to predict the direction of collision avoidance behavior. This model reflects the available figures and the margin of the expected threat when humans perform the collision avoidance actions. However, some discussion of these results are needed. The first is that the data used are AIS data. It has the advantage of providing a large number of vessel operation tracks. However, there is also the problem that data must be interpolated. And It is not only the change of direction that can be controlled by the vessel's evasive action, but also the use of engines [74]. No data directly certifying the use of the engine were entered into the AIS data. The data can estimate the deceleration of the speed; however, it is considered that this does not prove the direct use of the engine. Therefore, additional verification of changes in evasive maneuvering behavior owing to changes in ship speed using engines is required. In addition, the AIS data does not declare the qualifications of operators who have taken maneuvering action. According to Nakamura and Okada [75], the captain's maneuvering behavior is relatively concise, and in inexperienced navigators have been reported to postpone maneuvering judgment in a collision crisis. Therefore, for the model to be applied in practice, the qualifications of the operators who performed the collision-avoidance action must be reviewed as explanatory variables. Second, there was some interesting discussion regarding additional information that the operator obtains when avoiding a collision. This study used the essential information used by navigators to judge and figures from the collision avoidance algorithm and focused on basic collision avoidance predictions. However, it has been reported that additional figures should be considered for safety in restricted sea areas [45]. Therefore, a fixed object or Under Keel Clearance should also be considered when modeling for the strait or the area within the port limit. Third, the model is not a numerical prediction of a specific collision- avoiding course. To build the necessary model in an actual operating environment, it is necessary to have a numerical model that can predict not only the direction of avoidance, but also the course. Finally, the result that this model predicts is the prediction of the direction of collision avoidance. Currently, the registration of messages on collision avoidance behavior is being discussed in the framework of future AIS [76]. However, it is uncertain whether the equipment is forced to be set on all types of ships [77]. In addition, it has not been demonstrated whether the correct plan is transmitted from the ship. Therefore, considering the above points, the results

of this study are expected to prove helpful for the operators' decision-making.

Chapter 4

Modeling ship's encounter situation awareness result

4.1 Objective of this work

The aim of this work is to model the outcomes of the recognition of encounter situations by navigators who have identified the risk of collision in accordance with the COLREGs. The study is centered on the modeling of human situational awareness outcomes that differentiate between crossing and head-on scenarios. In accordance with the regulations outlined in the COLREGs, the process of overtaking can be ascertained by considering the angle of the stern light. In order to elucidate this procedure, data pertaining to human situation awareness outcomes in the context of potential collision scenarios was gathered. The necessary variables for the model were derived from the compiled data. Subsequently, a classifier model was developed to forecast human situation awareness outcomes, and its efficacy was subsequently validated.

The remainder of this work is as follows. Section 4.2 outlines the potential hazards and circumstances of collisions, and details the interview scenarios, variable construction, and pre-processing procedures employed for data collection. Subsequently, The methodology including constructing and evaluating a support vector machine had described to explain the relationship between the obtainable variables and the situation aware results in the face of a collision. Section 4.3 provides an analysis of the collected data and the outcomes derived from the model estimation. Section 4.4 discusses the results.

4.2 Materials and methods

Figure 4.1 shows the flow of this work. To illustrate the proposed model, the risk of collision had defined. The rationale behind establishing a definition for the risk of collision lies in the need to assess human susceptibility to such incidents, prompting the implementation of situation awareness and information processing strategies to prevent collisions. However, the risk of collision is a subjective. Hence, a metric known as the collision risk index (CRI) was employed to measure the likelihood of collision. It has been reported that a CRI exceeding 0.5 indicates a significant risk of conflict [78]. First, matrices are constructed to represent the navigator's situation recognition results in relation to the defined risk of collision. Subsequently, a questionnaire is developed based on the constructed scenarios. Finally, the methods for data collection, pre-processing, model construction, and verification are outlined.

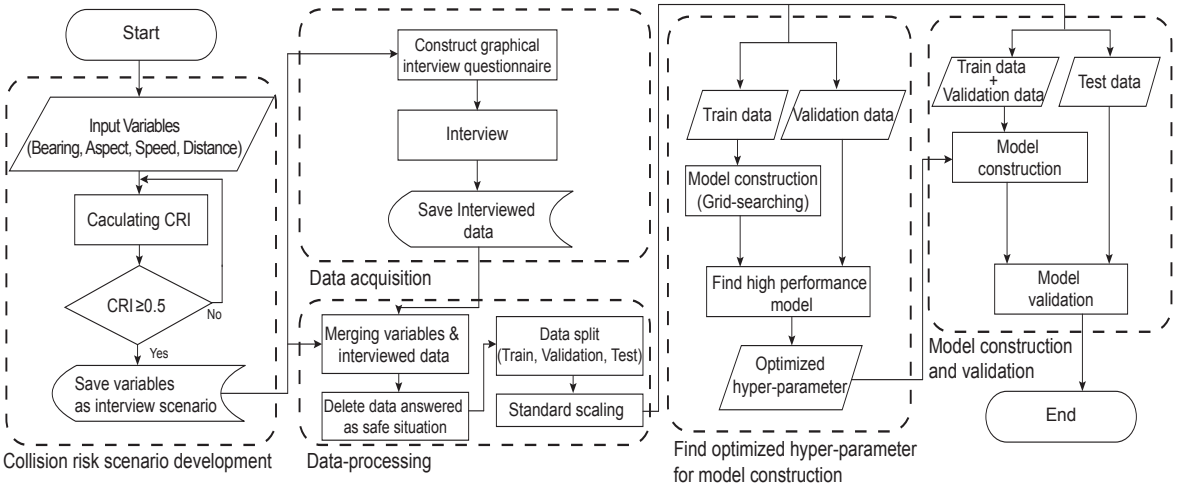

Figure 4.1. Flow charts of this work.

4.2.1 Risk of collision

This section outlines the numerical computation approach for determining the collision risk index during ship encounters. Subsequently, the process of conducting an interview scenario to gather the navigator's perception of the situation is detailed.

4.2.1.1 Collision Risk Index

In this research, a risk assessment index was employed to quantify the likelihood of collision. While various metrics exist for evaluating collision risk, the index described in the research conducted by Shaobo et al. [79] was utilized in this study. The reason for this decision was based on the variation in collision risk indexes reported in previous studies, which utilize different criteria to define head-on and crossing situations, resulting in the application of different weights. Consequently, it was deemed unsuitable for incorporation into this work. The necessary parameters for computing the indexes utilized in this work include DCPA, TCPA, distance (d), relative bearing (ψ_r), and speed ratio (K).

In the process described in Figure 4.1, The necessary parameters for computing the CRI were acquired. The CRI is determined through the conversion of the obtained parameters into utility functions. Equation 4.1 defines the collision risk indicators. The calculation involves the multiplication of the function of each parameter (U(x)) by its respective weight. The figures in Table 4.1 are the weights multiplied by the utility function. If the CRI exceeds 0.5, there is a potential for collision between the Own Ship (OS) and Target Ship (TS), necessitating the implementation of suitable measures by the OS to prevent the collision.

$$\text{CRI} = w_1\text{U}(\text{DCPA}) + w_2\text{U}(\text{TCPA}) + w_3\text{U}(d) + w_4\text{U}(\psi_r) + w_5\text{U}(K) \tag{4.1}$$

Table 4.1. Weight values for utility function of CRI.

Weight	w_1	w_2	w_3	w_4	w_5
	0.4	0.367	0.167	0.033	0.033

Equation 4.2 delineates a utility function (U(DCPA)) that pertains to the DCPA. This function transforms the DCPA into a numerical value ranging from 0 to 1, taking

into account the minimum passing distance (d_s) and the safe passing distance (d_p). Equation 4.3 outlines the computation of d_s based on the relative bearing (ψ_r).

$$\mathrm{U(DCPA)} = \begin{cases} 1 & , DCPA \leq d_s \\ \sin\Big[\dfrac{\pi}{d_p - d_s}(\mathrm{DCPA} - \dfrac{d_p + d_s}{2})\Big] & , d_s < \mathrm{DCPA} \leq d_p \\ 0 & , d_p \leq \mathrm{DCPA} \end{cases} \tag{4.2}$$

Here, d_p is twice d_s [79].

$$d_s = \begin{cases} 1.1 - \dfrac{\psi_r}{\pi} \times 0.2 & , 0 \leq \psi_r < \dfrac{5\pi}{8} \\ 1.0 - \dfrac{\psi_r}{\pi} \times 0.4 & , \dfrac{5\pi}{8} \leq \psi_r < \pi \\ 1.0 - \dfrac{2\pi - \psi_r}{\pi} \times 0.4 & , \pi \leq \psi_r < \dfrac{11\pi}{8} \\ 1.1 - \dfrac{2\pi - \psi_r}{\pi} \times 0.4 & , \dfrac{11\pi}{8} \leq \psi_r < 2\pi \end{cases} \tag{4.3}$$

Equation 4.4 delineates a utility function (U(TCPA)) representing a CRI's relationship with the TCPA. This function transforms the TCPA under specific circumstances.

$$\mathrm{U(TCPA)} = \begin{cases} 1 & , 0 \leq |\mathrm{TCPA}| \leq t_1 \\ \Big(\dfrac{t_2 - |\mathrm{TCPA}|}{t_2 - t_1}\Big)^2 & , t_1 < |TCPA| \leq t_2 \\ 0 & , t_2 \leq |TCPA| \end{cases} \tag{4.4}$$

Here, t_1 and t_2 of Equation 4.4 are calculated by Equations 4.5 and 4.6.

$$t_1 = \begin{cases} \dfrac{\sqrt{d_s^2 - \mathrm{DCPA}^2}}{V_r} & , \mathrm{DCPA} \leq d_s \\ \dfrac{d_s - \mathrm{DCPA}}{V_r} & , \mathrm{TCPA} > d_s \end{cases} \tag{4.5}$$

$$t_2 = \frac{\sqrt{d_p^2 - \mathrm{DCPA}^2}}{V_r} \tag{4.6}$$

Following this, the utility functions of the CRI pertaining to distance, direction, and speed ratio are derived as Equations 4.7, 4.8, and 4.9.

$$\mathrm{U}(d) = \begin{cases} 1 & ,0 \leq d \leq d_s \\ \left(\dfrac{d_p - d}{d_p - d_s}\right) & ,d_s < d \leq d_p \\ 0 & ,d_p < d \end{cases} \tag{4.7}$$

$$\mathrm{U}(\psi_r) = \frac{1}{2}\left[\cos\left(\psi_r - \frac{19\pi}{180}\right) + \sqrt{\frac{440}{289} + \cos^2\left(\psi_r - \frac{19\pi}{180}\right)}\right] - \frac{5}{17} \tag{4.8}$$

$$\mathrm{U}(K) = \left(1 + \frac{2}{K\sqrt{K^2 + 1 + 2K\sin\psi_o}}\right)^{-1} \tag{4.9}$$

4.2.1.2 Scenarios of collision

In order to collect data, it is essential to create a situation involving the potential for collision. This scenario was developed by constructing CRI values in matrix form, using numerical parameters to identify instances where the risk of collision is present. The horizontal axis of the matrix was based on the relative bearing of the TS in relation to the OS. In this study, the relative bearing was determined by the heading of the OS, ranging from -27 degrees to 27 degrees. Additionally, the aspect, defined as the angle at which the TS observes the OS, was limited to values between -25 degrees and 25 degrees. To create the questionnaire scenario, a collision risk index (CRI) of 0.5 or higher was calculated at randomly selected intervals for the aforementioned variables. The distance between the OS and the TS was fixed at 6 miles which reported as the distance to initiate collision avoidance procedures [80, 81]. The collision risk matrix was developed using the collision risk index outlined in section 4.2.2.1, considering three cases: when the OS is faster than the TS, when the speeds of the OS and TS are equal, and when the OS is slower than the TS. All cases are constructed based on the relative bearing, aspect, and fixed distance(6 nautical miles).

4.2.2 Acquisition of experimental data

In this section, a method for collecting data for model and for processing the collected data are described.

4.2.2.1 Interviewing

To carry out the interview, a scenario was created featuring an encounter with a CRI of 0.5 or greater, indicating a heightened risk of collision. The interview was then executed using this constructed scenario in the following manner: The survey was conducted from November 2022 to December 2022, with the aim of determining the type of encounter situation depicted in a given image (i.e., head-on, stand-on, give-away, or safe situation). The method employed for data collection was online, and the interviewees consisted of experienced navigators.

4.2.2.2 Data processing

The gathered data underwent a three-step procedure for processing:

- **Step 1** (integration of variables and survey data): The data necessary for the study were synthesized by amalgamating the scenarios presented during the interviews with the responses obtained from the interviewers. The presented scenario was utilized as a predictor, while the response outcome was utilized as a dependent variable.

- **Step 2** (variable construction): The explanatory variables chosen for analysis included the relative bearing, aspect, and speed ratio. Additionally, the result variable was categorized as head-on(0), give-away(1), and stand-on(2). It is important to note that data indicating a safe situation were excluded from model construction.

- **Step 3**(data pre-processing): The data undergo pre-processing to prepare for model development, which is essential as it impacts the model's performance [55]. In this work, each data point is split into training, validation, and test sets. Initially, the entire dataset is divided into training-validation and test sets, followed by a further division into training and validation sets at a ratio of 7:3. The predictors are then standardized, with standardization applied solely to the training data, without affecting the validation and test sets.

4.2.3 Modeling

The support vector machine is designed to estimate the correlation between the predictor obtained and the situational context resulting from the survey response. The model takes as input a variable derived from the process outlined in Section 4.2.2.2 and produces a prediction of situational awareness. The input and output data pairs were segregated into training-validation data and test data, with a division ratio of 7:3. Subsequently, the training-validation data were further divided into training and validation data at the same ratio, as the optimal hyperparameter is determined using grid search. (Box of Figure 4.1 named "Find optimized hyperparameter for model construction"). Ultimately, the final model was developed utilizing the most effective hyperparameters identified through the grid search. This section outlines the application of a support vector model to the constructed model, as well as the description of the hyperparameters. Lastly, the validation approach for the model is expounded upon.

4.2.3.1 Support Vector Machine

The Support Vector Machine (SVM) is a model designed to identify hyperplanes that effectively categorize given data [82]. SVMs have been noted for their strong generalization performance, as they strive to minimize training errors [83]. In SVM, the process of selecting a hyperplane involves finding the optimal solution, where the margin of the distance between the class data is maximized. The input data for the model is defined as $D = \{(x_1, y_1), (x_2, y_2) \cdots (x_i, y_i), y_i \in \{-1, 1\}\}$. The equation that defines the hyperplane for classifying classes based on their labels is $w \cdot x_i + b = 0$. Here, w represents the gradient of the hyperplane, x denotes the data's position on the hyperplane, and b signifies the bias. The separation hyperplane for the two classes of data is expressed as $w \cdot x_i + b \geq +1$(for $y_i = +1$) and $w \cdot x_i + b \leq -1$(for $y_i = -1$). Constraint term is derived by combining the two equations (Equation 4.10)

$$y_i(w \cdot x_i + b) \geq 1 \tag{4.10}$$

The support vectors refer to the data points located on the separation hyperplane of each class, and are characterized by the equation $w \cdot x_i + b = \pm 1$. The margin, which is the distance between the two support vectors, is calculated as $(2/\left\|w\right\|_2)$. The SVM is based on Equation 4.11, which aims to minimize the reciprocal of the distance, thereby maximizing the margin.

$$maxMargin = min\frac{1}{2}\|w\|_2 \tag{4.11}$$

Equations 4.10 and 4.11 are only available when they are entirely linearly separable. Therefore, Equations 4.12 and 4.13 are derived by adding terms that allow errors (ξ_i).

$$maxMargin = min\frac{1}{2}\|w\|_2^2 + C\sum_{i=1}^{n}\xi_i \tag{4.12}$$

$$y_i(w \cdot x_i + b) \geq 1 - \xi_i, i = 1, 2, \cdots, n \tag{4.13}$$

Here, ξ_i represents a measure of error, while C serves as a regulatory term that governs the extent of error regulation. A lower value of C permits a greater number of training errors, potentially leading to underfitting. Conversely, a higher value of C may result in overfitting due to the restriction of training errors.

Kernel transformations are employed to map predictors into higher dimensions, enabling the modeling of non-linear boundaries. These transformations encompass linear, polynomial (with d^{th} degree, where d is greater than or equal to 2), and Gaussian kernels, as defined by Equations 4.14 – 4.16.

$$K\langle x_1, x_2\rangle = \langle x_1, x_2\rangle \tag{4.14}$$

$$K\langle x_1, x_2\rangle = (a\langle x_1, x_2\rangle + b)^d \tag{4.15}$$

$$K\langle x_1, x_2\rangle = \exp\left(\frac{-\|x_1 - x_2\|_2^2}{2\sigma^2}\right) \tag{4.16}$$

4.2.3.2 Hyperparameters

The study employ the SVM models that encompasses linear, polynomial (2nd, 3rd), and Gaussian kernel. Each model is tailored to seek an optimal model by adjusting hyperparameters:

- **The linear model and polynomial models (2d, 3d)**: The regulatory parameter C has modified, with previous values of 0.001, 0.01, 0.1, 1, 10, 100, and 1000.
- **The Gaussian kernel model**: The parameters C and gamma, which regulate the Gaussian kernel dispersion, were modified. C was adjusted to the values of 0.001, 0.01, 0.1, 1, 10, and 100, while gamma was set to auto, 0.001, 0.01, 0.1, 1, 10, and 100. When gamma is set to auto, it is determined by the reciprocal of the number of predictors.
- **Grid search**: Grid search techniques were employed to efficiently determine the most suitable numerical value from a range of adjustable hyperparameters. This method involves pre-evaluating all potential hyperparameter combinations and identifying the optimal set through cross-validation. It is important to note that the test data should not be included in the grid search process. Consequently, the dataset was partitioned into three distinct subsets: training, validation, and test.

4.2.3.3 Verification of model

Various measures have been employed to assess the effectiveness of the constructed support vector machine models. Validation has been conducted using the Accuracy and F1 score, as well as the receiver operating characteristic (ROC) and area under the ROC curve (AUC) metrics. These measures are derived from the calculation of a confusion matrix [63]. The matrix represents the anticipated values of the labels derived from the actual labels. The calculation methods for most evaluation metrics are consistent with those reported in Chapter 3, subsection 2.3.3.. But, this study employed a multi-classification model. Figure 4.2 illustrates the confusion matrix for multi-class classification. In the assessment of multiple categories, metrics are computed using two methods, one of which is macro-averaging.

The precision and recall for each class in Figure 4.2 are computed independently. For classes 1, 2, and 3, the precision values are 5/7, 3/4, and 4/5, and the recall values are 5/5, 3/6, and 4/5, respectively. The macro-averaged precision and recall are obtained by averaging the precision and recall values for each class, resulting in values of 0.75 and 0.77, respectively. In contrast, micro-averaging involves calculating metrics using the overall positive and negative figures by constructing a confusion matrix for each class and summing the matrices. Figure 4.3 illustrates the development of a confusion matrix for each class using micro-averaging based on the data in Figure 4.2. The precision and recall achieved through micro-averaging is 0.75.

Python 3.7 and its libraries were used to build and validate the model [64, 65, 66, 67].

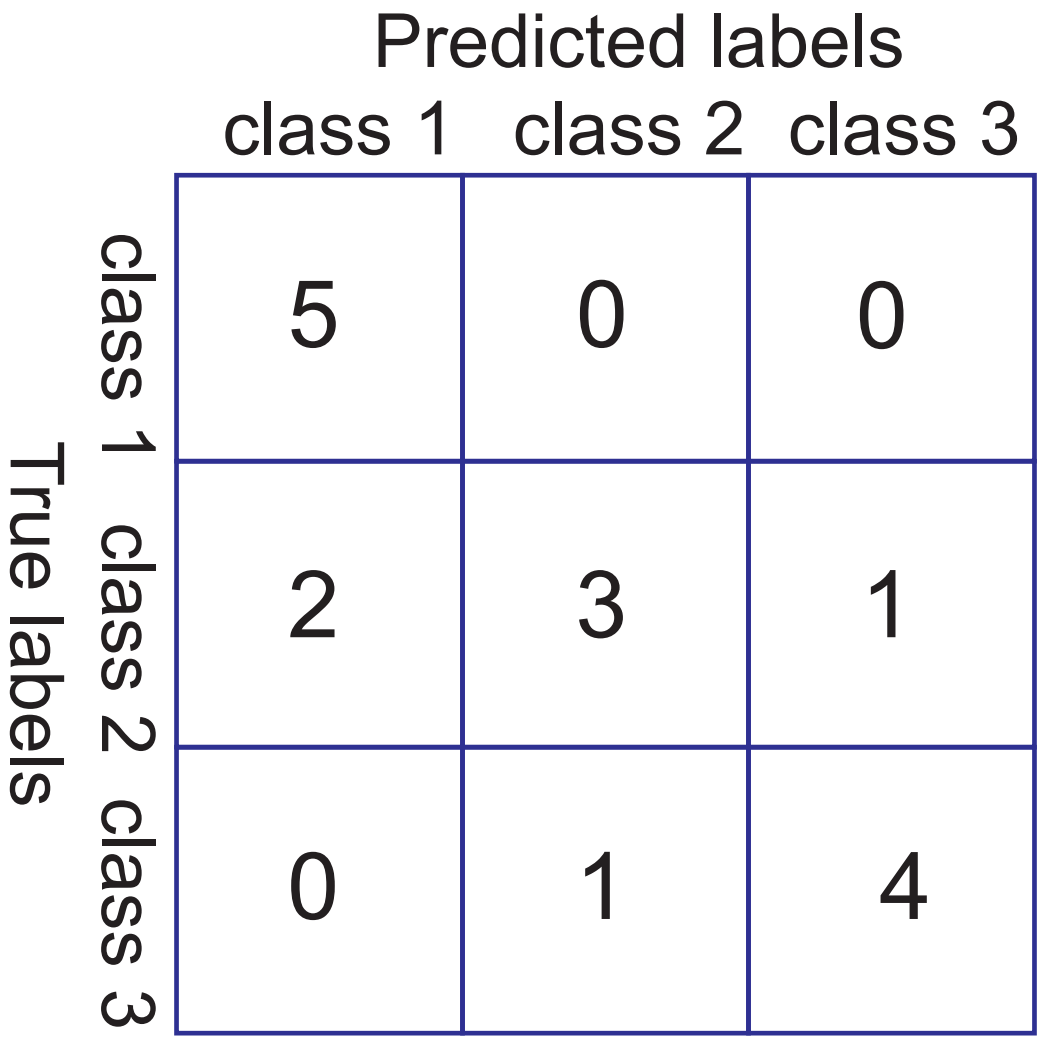

Figure 4.2. Illustration of the confusion matrix for Multi-class classification.

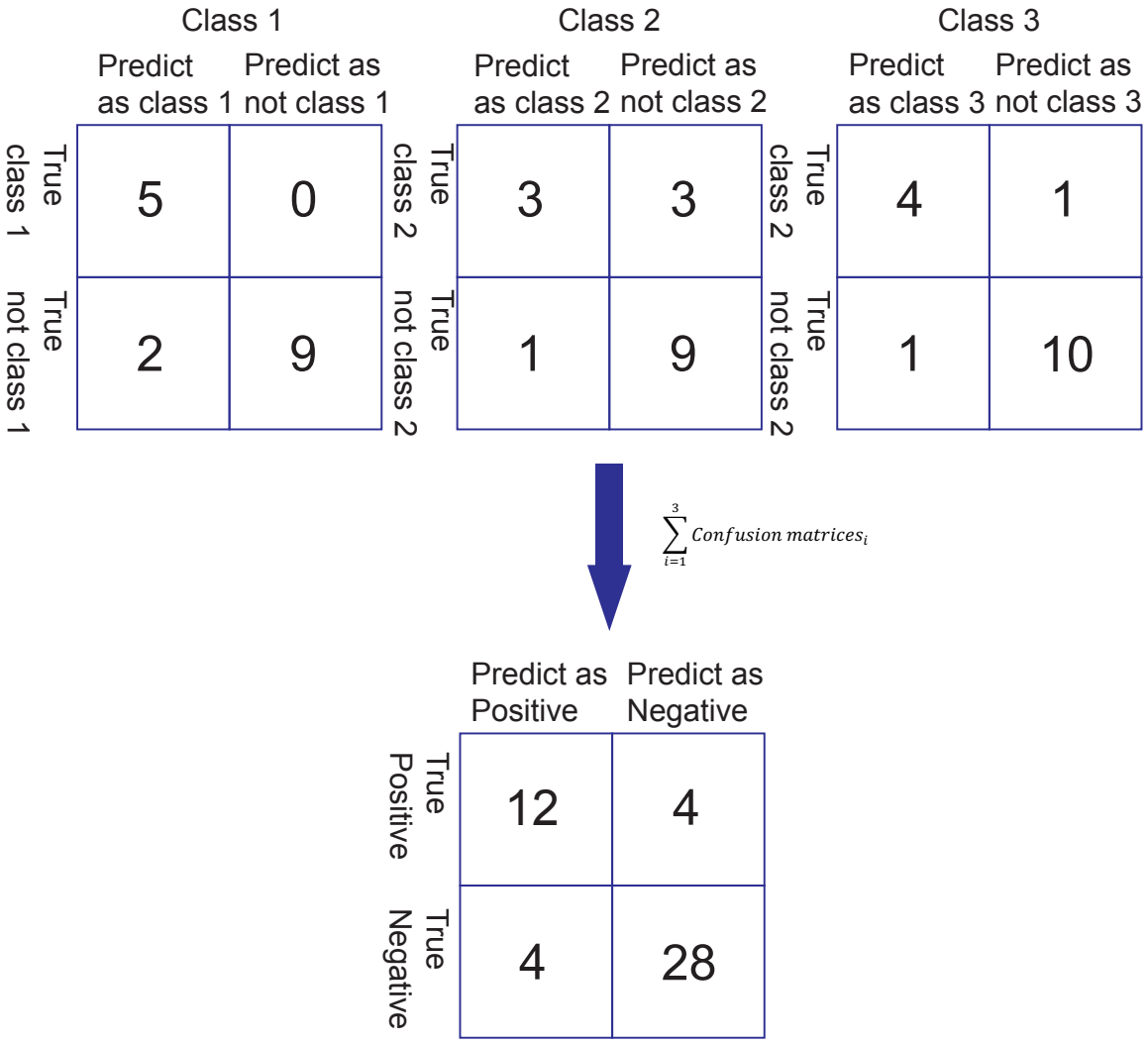

Figure 4.3. Illustration of the confusion matrix for micro-averaging.

4.3 Result

In this section, results of data acquisition and model construction are reported.

4.3.1 Results of data acquisition

In this subsection, the results of the construction of collision risk matrices required for the survey and survey are described.

4.3.1.1 Calculation results of Collision Risk

The scenario involving potential collision risk was represented as a matrix utilizing the CRI. The values outlined in subsection 4.2.1.2. were employed in the construction of the matrix, which was carried out in three distinct instances ($V_t < V_o$, $V_t = V_o$, and $V_t > V_o$). Figure 4.4 is a visualization of the constructed matrix as a heat map. In order to conduct interviews efficiently, some of the three scenarios was used as the final collision risk scenario.

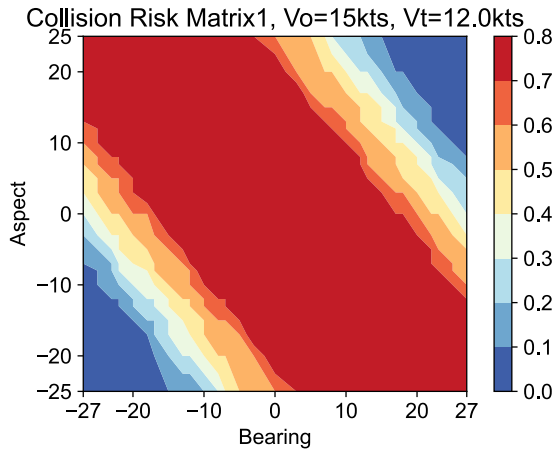

(a)

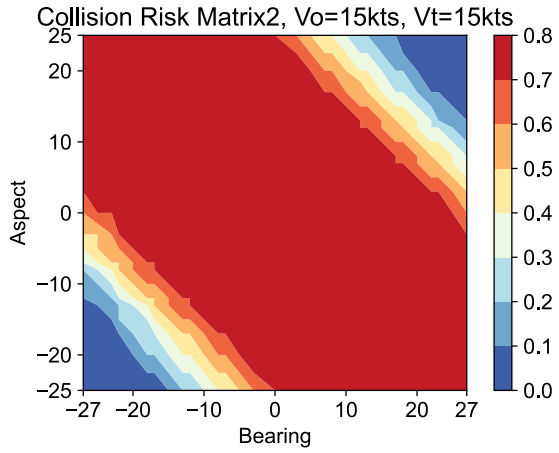

(b)

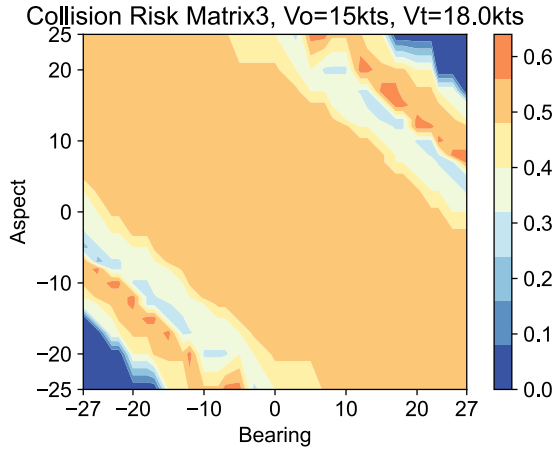

(c)

Figure 4.4. Visualization of collision risk matrices in case **(a)**, $V_t < V_o$, **(b)**, $V_t = V_o$, **(c)** $V_t > V_o$.

4.3.1.2 Results of data acquisition

The predictors and outcome variables utilized in constructing the model were obtained through the collection and pre-processing of data via surveys.
Interviewed data: It was collected from 36 mates(12 chief officers, 19 second officers, and 5 third officers) and 4 captains. In particular, 4767 data points were collected. Table 4.2 summarizes the characteristics and statistics of the variables used in the model. Figure 4.5 shows the distribution of predictors. Table 4.3 shows the correlation matrix between variables.

Table 4.2. Data description and statistical metrics.

Variable	Type	Unit	Count	Mean	Std	Min	Max
Relative bearing (ψ_r)	Continuous	Degree	4767	0.22	14.31	-27	27
Aspect	Continuous	Degree	4767	-0.03	11.98	-25	25
Speed rate (K)	Continuous	-	4767	1.00	0.17	0.75	1.25
Y	Categorical	-	4767	-	-	-	-

Table 4.3. Correlation matrix between the predictors.

	Relative Bearing(ϕ_r)	Aspect	Speed Rate(K)
Relative Bearing(ψ_r)	1		
Aspect	-0.63	1	
Speed Rate(K)	0.04	-0.01	1

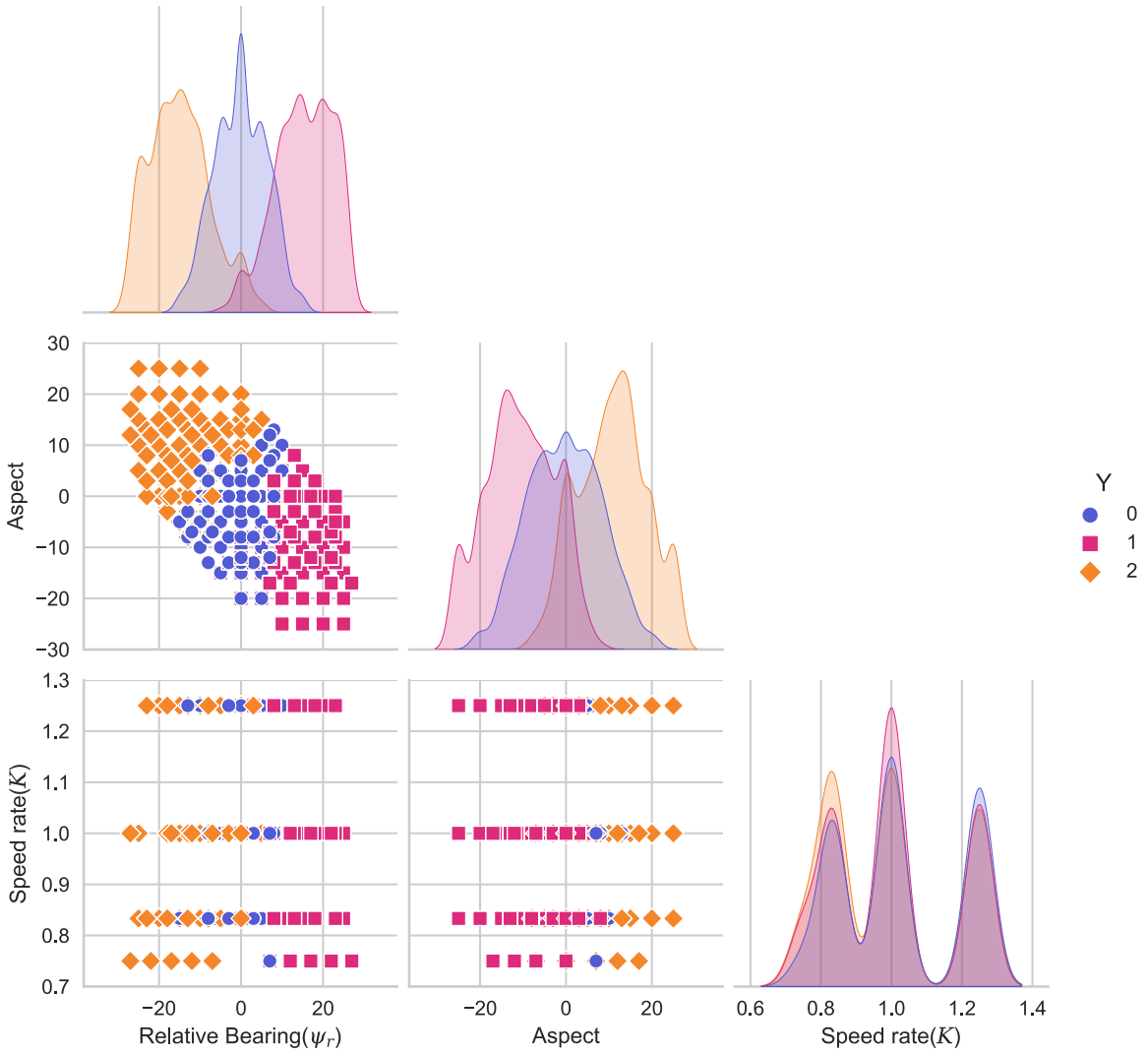

Figure 4.5. Distribution of the predictors. Set (Y) denote Head-on(0), Give- away(1), and Stand-on(2), respectively.

4.3.2 Results of modeling

The support vector machine model was utilized to develop the classification model. This section outlines the process of constructing the model and subsequently presents the findings of the verification process.

4.3.2.1 Estimation results of modeling

Each classification model utilized a support vector machine that was trained through the adjustment of the kernel and hyperparameters. The hyperparameters were selected through a search process aimed at achieving a high F1 score. The adjusted hyperparameters included the kernels, regulatory terms C, and gamma, which govern the bias of the Gaussian distribution for the Gaussian kernels. Table 4.4 shows the parameters of the optimized classification model. In model training, cross-validation was performed to prevent overfitting (5-fold).

Table 4.4. Estimation result of the optimal hyperparameters of the each kernel.

Model	Kernel	C	Gamma	Acc.	Precision	Recall	F1 Score	
					Macro	Macro	Macro	Micro
SVM	Linear	0.001	-	0.86	0.86	0.86	0.86	0.86
	Polynomial(2d)	10	-	0.62	0.61	0.63	0.61	0.62
	Polynomial(3d)	10	-	0.86	0.87	0.87	0.87	0.86
	Gaussian(RBF)	100	0.01	0.86	0.86	0.86	0.86	0.86

Here, C represents the regulatory terms, while Gamma serves as the parameter controlling the spread of the Gaussian kernel. Additionally, Acc. denotes the measure of accuracy.

4.3.2.2 Validation result of modeling

The confusion matrix for each model is shown in Table 4.5.

Table 4.5. Confusion matrices for high-performance by kernels of model.

Linear				Polynomial(2d)				Polynomial(3d)				Gaussian (RBF)			
True	Predicted			True	Predicted			True	Predicted			True	Predicted		
	0	1	2		0	1	2		0	1	2		0	1	2
0	320	35	21	0	343	20	13	0	335	20	21	0	302	41	33
1	43	366	0	1	49	243	117	1	47	362	0	1	33	376	0
2	70	0	337	2	81	174	152	2	74	0	333	2	60	0	347

Here, 0, 1, and 2 mean Head-on, Give-away, and Stand-on, respectively.

Furthermore, the study involved the computation of AUC scores and the acquisition of ROC curves, as depicted in Figure 4.6). With the exception of the polynomial (2d) model, the AUC scores obtained exceeded 0.9. Notably, the polynomial (3d) model demonstrated the highest accuracy and performance (F1 score) among the models developed. It is worth noting that this model did not exhibit overfitting, as evidenced by its training score of 0.88. Moreover, the ROC and AUC metrics also indicated a high performance level of 0.9 or above. Consequently, the polynomial (3d) model outperformed the other models under comparison.

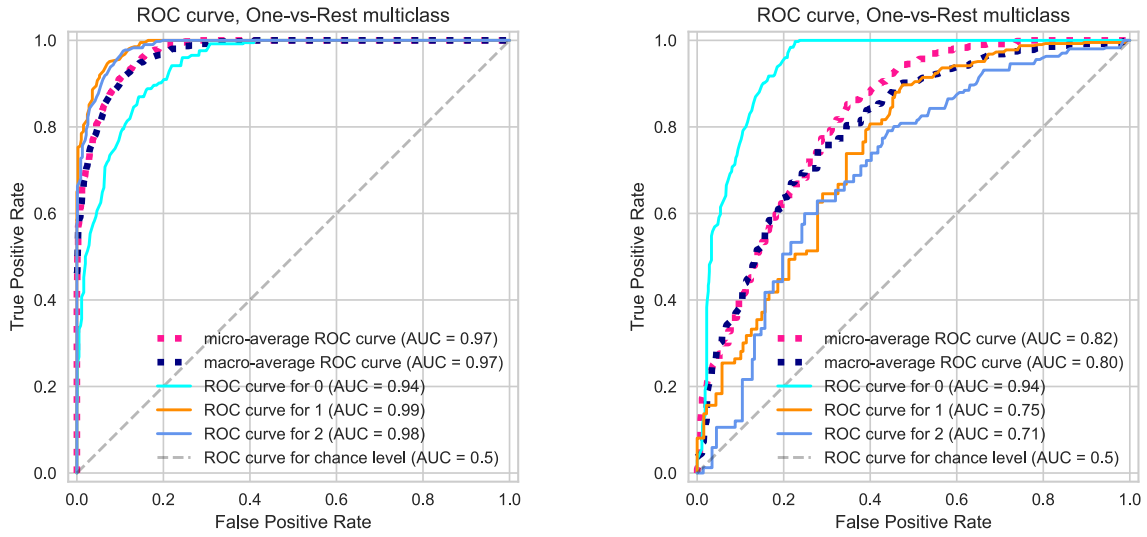

(a)

(b)

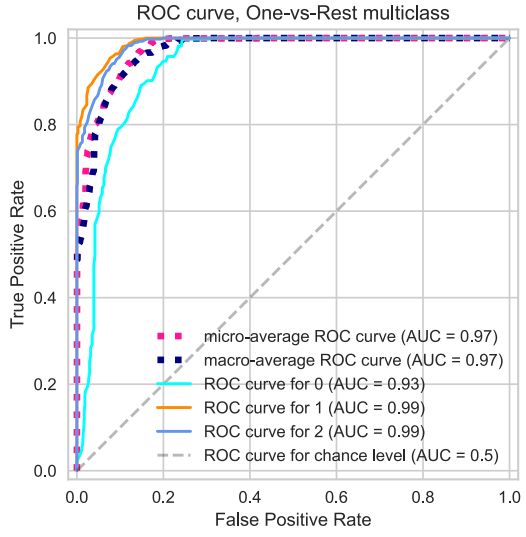

(c)

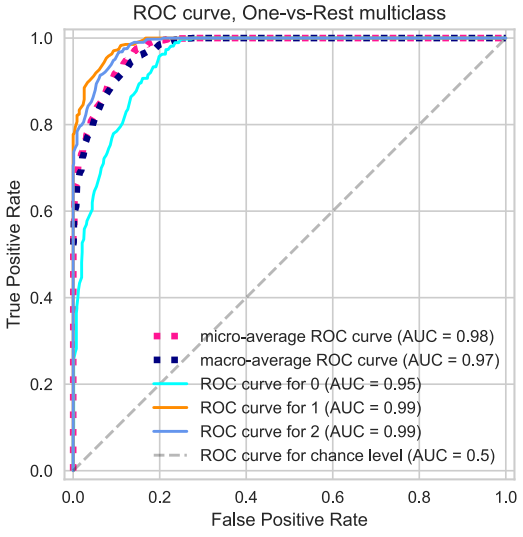

(d)

Figure 4.6. The receiver operating characteristic (ROC) curve and area under the curve (AUC) score of the different kernel functions are evaluated in the following cases: **(a)** Linear, **(b)** Polynomial (2nd degree), **(c)** Polynomial (3rd degree), and **(d)** Gaussian (RBF).

4.4 Discussion

This work utilized a support vector machine to construct a classification model for identifying encounter situations recognized by navigators. The primary contribution of this work was the development of a predictive model for identifying encounters recognized by navigation officers in situations with a risk of collision. This section provides an overview of the data, models, and results employed in the investigation. As outlined in Section 4.2, three numerical predictors were utilized: relative bearing, aspect, and speed ratio. These variables, as indicated in prior research, can be derived from the relative relationship between the OS and TS. In this study, the distance between the OS and TS was set at 6 miles, a distance known to trigger collision avoidance measures. The variables incorporated in the model were derived from surveys based on scenarios estimated using the CRI to indicate a collision risk in the relative relationship between the OS and TS. The CRI values are widely acknowledged as indicative of a risk of collision [78]. Hence, the decision to exclude the response to a specific question regarding safety from the model construction process was made. The survey involved 40 navigators, and despite this relatively small sample size, it was deemed feasible to construct the model due to the utilization of 4767 data points for its development and validation. To enable the model to accurately predict situational outcomes in collision-risk scenarios, it is imperative to establish a high-performing model based on human situational awareness findings. As detailed in Subsection 4.3.2, a model was devised to categorize situational recognition outcomes as head-on, give-away, and stand-on, and subsequently forecast these outcomes. The results presented in Subsection 4.3.2.1, along with the validation using ROC and AUC metrics and confusion matrix in Subsection 4.3.2.2, demonstrate the high performance of the model proposed in this study. Notably, the classifier's effectiveness is indicated by the ROC and AUC metrics scoring 0.9 or higher [73]. Method 1 provides the criteria established by Tam and Bucknall [18], Method 2 provides the criteria established by Hasegawa et al. [19] and Namgung [22], Method 3 provides the criteria established by Yoo and Lee [20], and Method 4 provides the criteria established by Zhang et al. [21]. Currently, Method 1 predominantly categorized the majority of cases as head-on situations. This is attributed to the classification standard of 22.5 degrees, which encompasses the widest range. Additionally, a segment of the study involved gathering the navigator's awareness results as a sample, and the methods employed for calculation were adjusted accordingly. This adjustment was necessitated by the

recognition of human fallibility and the impact of situational awareness, which are influenced by individual skills and technical expertise, and are presumed to have been accounted for in the reported findings.

Chapter 5

Conclusion

Modeling human situational awareness is a crucial element for maritime safety. This doctoral dissertation addressed the issue of operator's behavioral responses to the surrounding environment of ships at sea. To illustrate this, a predictive model based on machine learning was constructed to model ship's situational awareness outcomes. Two models were developed for this purpose. The first model is aimed at describing the relationship of evasion directions determined to escape situations where a collision seems imminent. This model was constructed using AIS data. The model was constructed using pre-processed variables derived from AIS data. The second model aims to describe the relationship between the conditions encountered by vessels in situations where a collision seems imminent and the situations interpreted and decided upon by operators. To construct this model, net based surveys were conducted with qualified navigators. Subsequently, the model was constructed using pre-processed variables derived from the survey results.

The explanatory variables needed for constructing both models are expected to influence the situational awareness and outcomes of vessel operators. These variables were selected from those reported to be used in analyzing the risk of vessels encountering potentially hazardous collision. The construction of these models utilized the commercial programming language Python (3.7) and relevant libraries.

Afterwards, the acquired data for each task was processed, and the variables obtained from that were used to train the models. Subsequently, the models were constructed, and their significance was validated in respectively.

- The first model, based on AIS data, successfully explained the relationship related to ship operators' evasion direction decisions.
- The second model, utilizing survey data based on responses from qualified navigators, effectively modeled the interpretation of vessel encounter situations by operators in potentially collision-prone scenarios.

- Both models captured and aided in understanding important variables in real navigation situations. Furthermore, they were trained with high numerical accuracy in representing human cognitive judgments.
- The hyperparameters optimizing the accuracy of each model were estimated. Using the grid-search method, the optimal hyperparameters for each model were identified based on the accuracy of the model.
- The practical usability of each model was validated. As a result of performing ROC-AUC metric validation, values of 0.9 or higher were obtained, confirming the usefulness of the proposed models.

Recently, there has been significant attention on the development of autonomous vessels. However, the focus has primarily been on the development of autonomous vessels themselves. Yet, after the successful development of autonomous vessels, attention will inevitably turn to the era of post-autonomous vessels, where encounters between autonomous and manned vessels cannot be overlooked. Therefore, it is anticipated that this model, when combined with automatic collision avoidance logic, could be utilized to predict the behavior of manned vessels by autonomous vessels in such encounters.

In this dissertation, only a classification model based on the outcomes of ship operators' behaviors was utilized to estimate the model. Remaining issues that should be addressed in future include the followings.

- It is necessary to develop a model that can predict specific numerical values even in various environmental conditions using regression models or equivalent models that yield similar results.
- As an extension of Chapter 3 of this dissertation, a model should be developed to explain human behavior patterns in Stand-on situations.
- This dissertation only models human situational awareness outcomes. In the future, it is essential to statistically analyze factors influencing situational awareness outcomes from a decision-making perspective.

Bibliography

[1] Japan Transport Safety Board. Japan transport safety board annual report of 2022. Japan Transport Safety Board, 2022, 145p.

[2] Japan Marine Accident Tribunal. Japan marine accident investigation report of 2022. Japan Marine Accident Tribunal, 2022, 39p.

[3] Japan Marine Accident Tribunal. Japan marine accident investigation report of 2021. Japan Marine Accident Tribunal, 2021, 39p.

[4] Japan Marine Accident Tribunal. Japan marine accident investigation report of 2020. Japan Marine Accident Tribunal, 2020, 39p.

[5] Y. Dong and D. M. Frangopol. Probabilistic ship collision risk and sustainability assessment considering risk attitudes. *Structural Safety*. 2015, 53, pp. 75–84.

[6] P. Sotiralis, N. P. Ventikos, R. Hamann, P. Golyshev, and A. Teixeira. Incorporation of human factors into ship collision risk models focusing on human centred design aspects. *Reliability Engineering & System Safety*. 2016, 156, pp. 210–227.

[7] R. Christian and H. G. Kang. Probabilistic risk assessment on maritime spent nuclear fuel transportation (part ii: Ship collision probability). *Reliability Engineering & System Safety*. 2017, 164, pp. 136–149.

[8] L. Zhang, H. Wang, Q. Meng, and H. Xie. Ship accident consequences and contributing factors analyses using ship accident investigation reports. *Proceedings of the Institution of Mechanical Engineers, Part O: Journal of risk and reliability*. 2019, 233(1), pp. 35–47.

[9] Y. Huang, L. Chen, P. Chen, R. R. Negenborn, and P. Van Gelder. Ship collision avoidance methods: State-of-the-art. *Safety science*. 2020, 121, pp. 451–473.

[10] H. Yu, Q. Meng, Z. Fang, J. Liu, and L. Xu. A review of ship collision risk assessment, hotspot detection and path planning for maritime traffic control in restricted waters. *The Journal of Navigation*. 2023, 75(6), pp. 1337-1363.

[11] J. Warot. A comment on the lisbon rules on compensation for damages in collision cases. *J. Mar. L. & Com.* 1987, 18, p. 583.

[12] P. Chen, Y. Huang, J. Mou, and P. Van Gelder. Probabilistic risk analysis for ship-ship collision: State-of-the-art. *Safety science*. 2019, 117, pp. 108–122.

[13] M. Li, J. Mou, L. Chen, Y. Huang, and P. Chen. Comparison between the collision avoidance decision-making in theoretical research and navigation practices. *Ocean Engineering*. 2021, 228, p. 108881.

[14] International Maritime Organization. COLREG: Convention on the International Regulations for Preventing Collisions at Sea 1972. London, UK, International Maritime Organization, 2002.

[15] Y. He, Y. Jin, L. Huang, Y. Xiong, P. Chen, and J. Mou. Quantitative analysis of colreg rules and seamanship for autonomous collision avoidance at open sea. *Ocean Engineering*. 2017, 140, pp. 281–291.

[16] J. I. Bowditch. American practical navigator. Blue Lake, CA, US, Paradise Cay Publications, 2010.

[17] Y. A. Ahmed, M. A. Hannan, M. Y. Oraby, and A. Maimun. Colregs compliant fuzzy-based collision avoidance system for multiple ship encounters. *Journal of Marine Science and Engineering*. 2021, 9(8), p. 790.

[18] C. Tam and R. Bucknall. Collision risk assessment for ships. *Journal of marine science and technology*. 2010, 15, pp. 257–270.

[19] K. Hasegawa, J. Fukuto, R. Miyake, and M. Yamazaki. An intelligent ship handling simulator with automatic collision avoidance function of target ships. *Proceedings of INSLC 17 – International Navigation Simulator Lecturer's Conference*. 2012, pp. 1-10.

[20] Y. Yoo and J.-S. Lee. Evaluation of ship collision risk assessments using environmental stress and collision risk models. *Ocean Engineering*. 2019, 191, p. 106527.

[21] W. Zhang, C. Yan, H. Lyu, P. Wang, Z. Xue, Z. Li, and B. Xiao. Colregs-based path planning for ships at sea using velocity obstacles. *IEEE Access*. 2021, 9, pp. 32613– 32626.

[22] H. Namgung. Local route planning for collision avoidance of maritime autonomous surface ships in compliance with colregs rules. *Sustainability*. 2021, 14(1), p. 198.

[23] Z. Pietrzykowski, P. Wołejsza, and P. Borkowski. Decision support in collision situations at sea. *The Journal of Navigation*. 2017, 70(3), pp. 447–464.

[24] C. Chauvin, J. Clostermann, and J.-M. Hoc. Situation awareness and the decision-making process in a dynamic situation: avoiding collisions at sea. *Journal of cognitive engineering and decision making*. 2008, 2(1), pp. 1–23.

[25] T. Statheros, G. Howells, and K. M. Maier. Autonomous ship collision avoidance navigation concepts, technologies, and techniques. *The journal of Navigation*. 2008, 61(1), pp. 129–142.

[26] R. Szlapczynski and J. Szlapczynska. Review of ship safety domains: Models and applications. *Ocean Engineering*. 2017, 145, pp. 277–289.

[27] H. Imazu, J. Fukuto, and M. Numano. Obstacle zone by target and its expression. *The Journal of Japan Institute of Navigation*. 2002, 107, pp. 191–197.

[28] J. Kayano, H. Imazu, H. Tamaru, and T. Fujisaka. On the prediction of ship's motion for ozt by using kalman filter. *The Journal of Japan Institute of Navigation*. 2010, 123, pp. 129–134.

[29] R. Sawada, K. Sato, and T. Majima. Automatic ship collision avoidance using deep reinforcement learning with lstm in continuous action spaces. *Journal of Marine Science and Technology*. 2021, 26, pp. 509–524.

[30] P. Fiorini and Z. Shiller. Motion planning in dynamic environments using velocity obstacles. *The international journal of robotics research*. 1998, 17(7), pp. 760–772.

[31] Y. Kuwata, M. T. Wolf, D. Zarzhitsky, and T. L. Huntsberger. Safe maritime autonomous navigation with colregs, using velocity obstacles. *IEEE Journal of Oceanic Engineering*. 2013, 39(1), pp. 110–119.

[32] Y. Huang, P. Van Gelder, and Y. Wen. Velocity obstacle algorithms for collision prevention at sea. *Ocean Engineering*. 2018, 151, pp. 308–321.

[33] J. Kearon. Computer programs for collision avoidance and traffic keeping conference on mathematical aspects on marine traffic. 1997.

[34] J. Lisowski. Determining the optimal ship trajectory in collision situation. *Proceedings of the IX International Scientific and Technical Conference on Marine Traffic Engineering*. 2001, pp. 192–201.

[35] Y. Ren, J. Mou, Q. Yan, and F. Zhang. Study on assessing dynamic risk of ship collision. *ICTIS 2011: Multimodal Approach to Sustained Transportation System Development: Information, Technology, Implementation*. 2011, pp. 2751–2757.

[36] Q. Xu and N. Wang. A survey on ship collision risk evaluation. *Promet-Traffic&Transportation*. 2014, 26(6), pp. 475–486.

[37] Y. Fujii and K. Tanaka. Traffic capacity. *The Journal of navigation*. 1971, 24(4), pp. 543–552.

[38] E. M. Goodwin. A statistical study of ship domains. *The Journal of navigation*. 1975, 28(3), pp. 328–344.

[39] T. Coldwell. Marine traffic behaviour in restricted waters. *The Journal of Navigation*. 1983, 36(3), pp. 430–444.

[40] J.-B. Yim, D.-S. Kim, and D.-J. Park. Modeling perceived collision risk in vessel encounter situations. *Ocean Engineering*. 2018, 166, pp. 64–75.

[41] Z. Chen, J. Xue, C. Wu, L. Qin, L. Liu, and X. Cheng. Classification of vessel motion pattern in inland waterways based on automatic identification system. *Ocean Engineering*. 2018, 161, pp. 69–76.

[42] J. Xue, C. Wu, Z. Chen, P. Van Gelder, and X. Yan. Modeling human-like decision making for inbound smart ships based on fuzzy decision trees. *Expert Systems with Applications*. 2019, 115, pp. 172–188.

[43] J. Xue, P. Van Gelder, G. Reniers, E. Papadimitriou, and C. Wu. Multi-attribute decision-making method for prioritizing maritime traffic safety influencing factors of autonomous ships' maneuvering decisions using grey and fuzzy theories. *Safety Science*. 2019, 120, pp. 323–340.

[44] J. Xue, Z. Chen, E. Papadimitriou, C. Wu, and P. Van Gelder. Influence of environmental factors on human-like decision-making for intelligent ship. *Ocean Engineering*. 2019, 186, p. 106060.

[45] W. Galor. The role of navigational risk assessment during ship's manoewring in limited waters. *Journal of KONES*. 2009, 16(2), pp. 117–124.

[46] A. J. Swift. Bridge team management: a practical guide. 2nd edition, Nautical Institute, 2004, 110p.

[47] Oil Companies International Marine Forum. "Ship inspection report (sire) programme vessel inspection questionnaires (VIQ) 7". https://www.ocimf.org/programmes/sire/. (accessed on 2022-11-27).

[48] H. Imazu. Computation of ozt by using collision course. *Navigation of Japan Institute of Navigation*. 2014, 188, pp. 78–81.

[49] G. Bennett. Practical rhumb line calculations on the spheroid. *The Journal of Navigation*. 1996, 49(1), pp. 112–119.

[50] C. Veness. "Calculate distance, bearing and more between latitude/longitude points". http://www.movable-type.co.uk/scripts/latlong.html/. (accessed on 2022-05-24).

[51] F. Xiao, H. Ligteringen, C. Van Gulijk, and B. Ale. Comparison study on ais data of ship traffic behavior. *Ocean Engineering*. 2015, 95, pp. 84–93.

[52] International Maritime Organization. Model course 1.34 Automatic Identification Systems. London, UK, International Maritime Organization, 2006.

[53] Japan Meteorological Agency. "Tables of historical weather data". https://www.data.jma.go.jp/gmd/risk/obsdl/. (accessed on 2022-05-24).

[54] International Maritime Organization. Adoption of New and Amended Performance Standards for Navigational Equipment. London, UK, International Maritime Organization, 1998.

[55] S. A. Alasadi and W. S. Bhaya. Review of data preprocessing techniques in data mining. *Journal of Engineering and Applied Sciences*. 2017, 12(16), pp. 4102–4107.

[56] L. Rokach. Ensemble-based classifiers. *Artificial intelligence review*. 2010, 33, pp. 1–39.

[57] D. Opitz and R. Maclin. Popular ensemble methods: An empirical study. *Journal of artificial intelligence research*. 1999, 11, pp. 169–198.

[58] G. J. Briem, J. A. Benediktsson, and J. R. Sveinsson. Multiple classifiers applied to multisource remote sensing data. *IEEE transactions on geoscience and remote sensing*. 2002, 40(10), pp. 2291–2299.

[59] L. Breiman. Bagging predictors. *Machine learning*. 1996, 24, pp. 123–140.

[60] E. Bauer and R. Kohavi. An empirical comparison of voting classification algorithms: Bagging, boosting, and variants. *Machine learning*. 1999, 36, pp. 105–139.

[61] Y. Freund and R. E. Schapire. A decision-theoretic generalization of on-line learning and an application to boosting. *Journal of computer and system sciences*. 1997, 55(1), pp. 119–139.

[62] A. Kadiyala and A. Kumar. Applications of python to evaluate the performance of decision tree-based boosting algorithms. *Environmental Progress & Sustainable Energy*. 2018, 37(2), pp. 618–623.

[63] J. Han, M. Kamber, and J. Pei. Data mining concepts and techniques. 3rd edition, University of Illinois at Urbana-Champaign Micheline Kamber Jian Pei Simon Fraser University, 2012, 744p.

[64] G. Van Rossum and F. Drake. Python 3 Reference Manual. Scotts Valley, CA, US, CreateSpace, 2009.

[65] W. McKinney. Data structures for statistical computing in python. *Proceedings of the 9th Python in Science Conference*. 2010, vol. 445(1), pp. 51–56.

[66] F. Pedregosa, et al. Scikit-learn: Machine learning in python. *The Journal of machine Learning research*. 2011, 12, pp. 2825–2830.

[67] C. R. Harris, et al. Array programming with numpy. *Nature*. 2020, 585(7825), pp. 357–362.

[68] S. Kuwahara, et al. Research and development of collision risk decision method for safe navigation and its verification. ClassNK technical journal. 2021, 3, pp. 1–11.

[69] W. Schiff and M. L. Detwiler. Information used in judging impending collision. *Perception*. 1979, 8(6), pp. 647–658.

[70] I. T. Feldstein. Impending collision judgment from an egocentric perspective in real and virtual environments: a review. *Perception*. 2019, 48(9), pp. 769–795.

[71] O. Sagi and L. Rokach. Ensemble learning: A survey. *Wiley Interdisciplinary Reviews: Data Mining and Knowledge Discovery*. 2018, 8(4), p. e1249.

[72] L. Breiman. Random forests. *Machine learning*. 2001, 45, pp. 5–32.

[73] M. P. Muller, G. Tomlinson, T. J. Marrie, P. Tang, A. McGeer, D. E. Low, A. S. Det- sky, and W. L. Gold. Can routine laboratory tests discriminate between severe acute respiratory syndrome and other causes of community-acquired pneumonia?. *Clinical infectious diseases*. 2005, 40(8), pp. 1079–1086.

[74] P. Mizythras, C. Pollalis, E. Boulougouris, and G. Theotokatos. A novel decision support methodology for oceangoing vessel collision avoidance. *Ocean Engineering*. 2021, 230, p. 109004.

[75] S. Nakamura and N. Okada. Development of automatic collision avoidance system and quantitative evaluation of the manoeuvring results. *TransNav: International Journal on Marine Navigation and Safety of Sea Transportation*. 2019, 13(1), pp. 133–141.

[76] International Association of Marine Aids to Navigation and Lighthouse Authorities. "VHF data exchange system (VDES) overview (g1117)." https://www.ocimf.org/programmes/sire/. (accessed on 2022-12-01).

[77] F. Lázaro, R. Raulefs, W. Wang, F. Clazzer, and S. Plass. Vhf data exchange system (vdes): an enabling technology for maritime communications. *CEAS space Journal*. 2019, 11(1), pp. 55–63.

[78] N. Im and T. N. Luong. Potential risk ship domain as a danger criterion for real-time ship collision risk evaluation. *Ocean Engineering*. 2019, 194, p. 106610.

[79] W. Shaobo, Z. Yingjun, and L. Lianbo. A collision avoidance decision-making system for autonomous ship based on modified velocity obstacle method. *Ocean Engineering*. 2020, 215, p. 107910.

[80] A. Cockcroft. A manoeuvring diagram for avoiding collisions at sea. *The Journal of Navigation*. 1972, 25(1), pp. 105–107.

[81] Y.-S. Lee, J.-M. Park, and Y.-J. Lee. A study on the initial action of navigators to avoid risk of collision at sea. *Journal of navigation and port research*. 2014, 38(4), pp. 327–333.

[82] B. E. Boser, I. M. Guyon, and V. N. Vapnik. A training algorithm for optimal margin classifiers. *Proceedings of the fifth annual workshop on Computational learning theory*. 1992, pp. 144–152.

[83] V. Vapnik. The nature of statistical learning theory. Berlin/Heidelberg, Germany, Springer science & business media, 1999.

Appendix A

The outputs of the proposed models

In the main body of the doctoral dissertation, significant attention was given to constructing goal models for each chapter and validating the validity of the models. Therefore, in this appendix, the outputs of the models constructed in Chapter 3 and Chapter 4 are described. To explain the outputs of the models, an overview of the entire model is provided. Subsequently, the results of the model when data is inputted under given variables are reported.

A.1 The overview of the model illustrated in Chapter 3

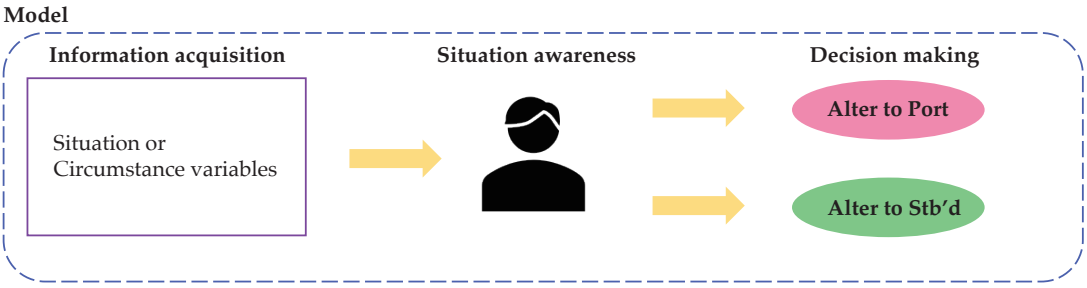

Figure A.1. Overview of model constructed in Chapter 3

The object of Chapter 3 was to construct a model that models the direction of avoidance action of the vessel, which is the answer to human behavior in situations where the risk of collision exists. Here the behavior of human include the human errors.

The figure A.1 illustrates the process by which trained ship operators process information and derive situational awareness outcomes. When sensing a crisis of col-

lision, the operator gathers situational information and performs situational awareness. Subsequently, they engage in actions to choose evasion directions. These flows have traditionally been performed by humans and are susceptible to human errors.

A.2 The Output of the model illustrated in Chapter 3

The table A.1 describes the model's predicted outcomes when variables are inputted using the trained model. The model's predicted outcomes are explained in the Y column of the table A.1.

Table A.1. Example of prediction result of optimal model constructed in chapter 3.

Speed rate	Size rate	DCPA	TCPA	Aspect	d_{ozt}	θ_{ozt}	Y
2.2	1.8	1.31	0.42	-9.6	7.88	-6.64	Port
1.7	1.5	0.76	0.35	-19.9	7.21	-11.12	Starboard
1.3	1.9	1.26	0.44	-8.9	8.99	-12.17	Starboard
1.3	0.6	0.91	0.47	-6.0	7.45	-2.92	Port
0.8	2.2	1.05	0.25	-8.4	3.56	-30.37	Starboard
0.7	1.1	1.28	0.48	-6.1	6.54	-5.79	Port
0.9	1	0.62	0.40	-2.3	4.54	-1.55	Port
0.6	1.2	0.70	0.39	-6.5	3.5	-6.73	Port
0.6	0.6	1.39	0.47	13	6.18	14.65	Port
0.6	0.5	0.16	0.44	1.5	5.15	4.59	Starboard
0.5	1.4	0.47	0.48	2.4	6.06	11.5	Starboard
0.4	0.4	0.36	0.29	-0.1	2.18	0.13	Starboard

A.3 The overview of the model illustrated in Chapter 4

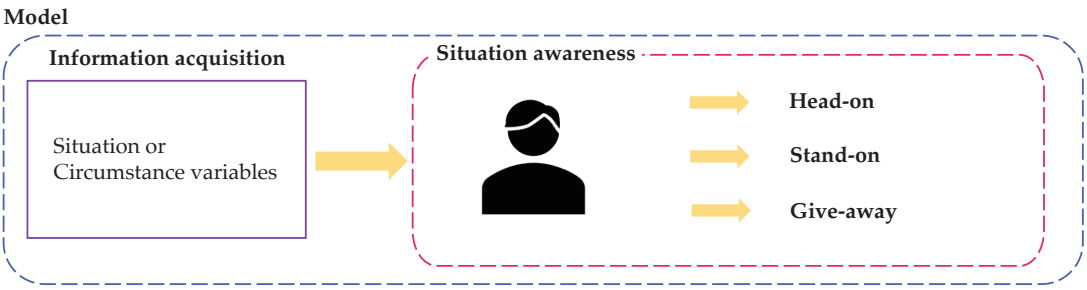

Figure A.2. Overview of model constructed in Chapter 4

The objective of the work in Chapter 4 was to model situational awareness outcomes of ships operator who trained about regulations the COLREG.

The figure A.2 depicts the process by which trained ship operators process information and derive situational awareness outcomes. When sensing the risk of collision, the operator gathers situational information and performs situational awareness. Subsequently, they engage in analysis to define the encounter situation. The encounter situation is interpreted by humans who have learned the regulations of COLREG, which do not clearly define numerical values for differentiating encounter situations.

A.4 The Output of the model illustrated in Chapter 4

The table A.2 describes the model's predicted outcomes when variables are inputted using the trained model. The model's predicted outcomes are explained in the Y column of the table A.2.

Table A.2. Example of prediction result of optimal model constructed in chapter 4.

Relative bearing	Aspect	Y	Relative bearing	Aspect	Y	Relative bearing	Aspect	Y
-18	0	Stand-on	-5	-15	Head-on	25	-5	Give-away
-18	3	Stand-on	-5	-10	Head-on	27	-17	Give-away
-18	8	Stand-on	-5	-5	Head-on	7	7	Head-on
-18	13	Stand-on	-5	0	Head-on	7	12	Head-on
-17	0	Stand-on	-5	5	Head-on	8	-13	Give-away
-17	7	Stand-on	-5	10	Head-on	8	-8	Give-away
-17	17	Stand-on	-5	20	Stand-on	8	-3	Head-on
-15	-5	Stand-on	-3	-13	Head-on	8	0	Head-on
-15	0	Stand-on	-3	-8	Head-on	8	3	Head-on
-15	5	Stand-on	-3	-3	Head-on	8	8	Head-on
-15	10	Stand-on	-3	0	Head-on	8	13	Head-on
-15	15	Stand-on	-3	3	Head-on	10	-25	Give-away
-15	20	Stand-on	-3	8	Head-on	10	-20	Give-away
-15	25	Stand-on	-3	13	Head-on	10	-15	Give-away
-13	-8	Head-on	0	-20	Head-on	10	-10	Give-away
-13	-3	Head-on	0	-15	Head-on	10	-5	Give-away
-13	0	Stand-on	0	-10	Head-on	10	0	Head-on
-13	3	Stand-on	0	-5	Head-on	10	5	Head-on
-13	8	Stand-on	0	5	Head-on	10	10	Head-on
-13	13	Stand-on	0	10	Head-on	12	-17	Give-away
-12	-7	Head-on	0	15	Head-on	12	-7	Give-away
-12	7	Stand-on	0	17	Stand-on	12	0	Give-away
-12	12	Stand-on	0	20	Stand-on	13	-13	Give-away
-12	17	Stand-on	3	-13	Head-on	13	-8	Give-away
-10	-10	Head-on	3	-8	Head-on	13	-3	Give-away
-10	-5	Head-on	3	-3	Head-on	13	0	Give-away
-10	0	Head-on	3	0	Head-on	13	3	Give-away
-10	5	Stand-on	3	3	Head-on	13	8	Head-on
-10	10	Stand-on	3	8	Head-on	15	-25	Give-away
-10	15	Stand-on	3	13	Head-on	15	-20	Give-away
-10	20	Stand-on	5	-20	Give-away	15	-15	Give-away
-10	25	Stand-on	5	-15	Give-away	15	-10	Give-away
-8	-13	Head-on	5	-10	Head-on	15	-5	Give-away
-8	-8	Head-on	5	-5	Head-on	15	0	Give-away
-8	-3	Head-on	5	0	Head-on	15	5	Give-away
-8	0	Head-on	5	5	Head-on	17	-12	Give-away
-8	3	Head-on	5	10	Head-on	17	0	Give-away
-7	-7	Head-on	5	15	Head-on	18	-13	Give-away
-7	0	Head-on	7	-7	Head-on	18	-8	Give-away

Acknowledgments

As important as the achievements of my research are, it is crucial to express gratitude to everyone who has helped me throughout my long-term Ph.D. course. I must emphasize that completing a Ph.D. degree would have been impossible without a significant amount of support, whether direct or indirect, technical, financial, or emotional. At the same time, it is challenging to mention all those who have provided such valuable support. Therefore, I apologize in advance to those who are not mentioned here, but please know that your assistance and contribution are greatly appreciated.

Firstly, I would like to express my deepest gratitude to my advisors, Professor Hitoi Tamaru, Tadasuke Furuya, and Associate Professor Jun Kayano, for their guidance, care, patience, and for providing me with an excellent research environment. Additionally, I would like to thank several graduate students whose friendships have helped me become a better researcher.

And I owe special thanks to my former advisor, Ruri Shoji, the president of the National Institute of Maritime, Port, and Aviation Technology, for her continuous guidance, care, and encouragement. Without her, I couldn't have begun the Ph.D. course. Furthermore, I have been deeply inspired and motivated by her attitude as a researcher and her dedication to research.

This work would not have been possible without the financial and educational support from the JST project (TUMSAT-SPRING). They have been extremely supportive of me throughout my Ph.D. course.

Finally, I want to express my special gratitude to my parents for their unwavering support and encouragement. They have always been a tremendous source of inspiration to me and have supported me in every endeavor, no matter what it was. They have provided me with countless opportunities, for which I will be forever grateful.

Without such incredible people supporting me, I doubt that I would be where I am today.